eLife

Reviewed Preprint
v1 • March 18, 2026
Not revised

For correspondence:
axin@andrew.cmu.edu
gabriel.loewinger@nih.gov

Competing interests: No competing interests declared

Funding: See page 21

Reviewing editor: Philip Boonstra, University of Michigan, United States

Capturing instantaneous neural signal-behavior relationships with concurrent functional mixed models

Al W Xin[1,3], **Erjia Cui**[2], **Francisco Pereira**[1], **Gabriel Loewinger**[1]

[1]Machine Learning Core, National Institute of Mental Health, Bethesda, United States • [2]Division of Biostatistics and Health Data Science, University of Minnesota, Minneapolis, United States • [3]Department of Statistics and Data Science, Carnegie Mellon University, Pittsburgh, United States

eLife Assessment

This **valuable** work extends a previously published regression framework for trial-aligned photometry data incorporating functional variables. However, the evidence is generally **incomplete**, due to the way that within-trial changes in variables have been incorporated into an inherently cross-trial analysis framework, which will limit general adoption. The ideas in this work will be of interest to researchers analyzing photometry signals.

https://doi.org/10.7554/eLife.109428.1.sa4

Abstract

We previously proposed an analysis framework for fiber photometry data based on functional linear mixed models (FLMMs). Functional LMMs allow modeling associations between photometry traces and trial-specific scalar values like behavioral summaries and session number, while also accounting for between-animal heterogeneity. Here, we extend the method to concurrent FLMMs (cFLMMs), a method that can fit the instantaneous relationship between functional outcomes and functional covariates. Concurrent FLMMs enable testing of how the photometry signal is associated with, for example, a behavioral variable that evolves across within-trial timepoints (e.g. animal speed). cFLMMs can also model the relationship between the photometry signal and covariates in experiments with variable trial lengths (e.g., in studies where trials end when an animal responds). We illustrate the application of cFLMMs on two published studies and show the method can identify signal–behavior associations in analyses not possible with FLMMs. We find that analyzing photometry–behavior associations based on behavioral summaries (e.g., latency-to-response, average lick rate) can lead to misleading conclusions. We published our method in the `fastFMM` package, available as an R package through GitHub (*https://github.com/awqx/fastFMM*).

Introduction

Fiber photometry allows for measurement of neural activity in vivo, and is useful for its high temporal resolution and neurotransmitter specificity. In Loewinger et al. (2025), we demonstrated that *functional linear mixed models* (FLMMs) can effectively identify individual-level and trial-level temporal patterns in fiber photometry data. FLMMs provide key advantages over standard methods, including modeling instantaneous photometry signals at all the time points in each trial, providing hypothesis tests at each trial timepoint, and controlling for subject-specific effects. However, FLMMs are limited to capturing photometry dynamics with respect to scalar covariates. That is, FLMM can incorporate covariates that vary between trials, but they can only take a single value per trial, e.g., trial number, session, or behavioral summaries like latency-to-press, or total button presses during the trial. Limiting functional analysis to scalar covariates can coarsen available data and obscure time-varying associations between the signal and covariates.

In this work, we extend our method to *concurrent FLMMs* (cFLMMs), which can capture relationships with *functional covariates*, i.e. covariates that change across timepoints within one trial. Functional covariates can include (1) behavioral measures, like a subject's speed, position, or actions, (2) changing experimental conditions, such as differing trial lengths or reward periods, or (3) an additional neural signal. Concurrent functional linear mixed modeling is one of a number of possible strategies for jointly modeling functional covariates and functional outcomes. For example, one could instead apply function-on-function regression (Scheipl et al.,2016), but we are not aware of longitudinal versions of this method. We opted for concurrent FLMMs because they can model instantaneous associations between the output and functional covariate (e.g., the relationship between the photometry signal and behavior at a specific within-trial timepoint) in longitudinal datasets.

> ***Box 1.***
>
> **Procedure for fitting a concurrent FLMM.**
>
> We developed a procedure that fits a concurrent FLMM in three steps:
>
> 1. **Fit univariate models**. Separate linear mixed models are fit at every point along the *functional domain*. That is, if there are *L* longitudinal data points, *L* different linear mixed models will be produced.
> 2. **Smooth coefficients**. Aggregate and smooth the coefficient estimates for the linear models over the functional domain using penalized splines (Cui et al. (2022); Loewinger et al. (2025)).
> 3. **Build joint confidence intervals**. Combine the within-timepoint variance and the between-timepoint covariance to create confidence bands around the smoothed estimates from Step 2.
>
> The procedure for fitting a concurrent FLMM and a non-concurrent FLMM are similar and differ primarily in the calculation of joint confidence intervals in Step 3 (Concurrent FLMM estimation). In fact, if the functional covariate of interest is a scalar constant across the domain, the models fit by the concurrent and non-concurrent procedure are identical.

By introducing cFLMMs in the photometry context, we aim to demonstrate that they can capture temporal dynamics on real experimental data, similar to our experiments with *non-concurrent* FLMMs (ncFLMMs). Our examples are chosen to illustrate particular cases where concurrent modeling can provide insight into questions where modeling scalar covariates in ncFLMMs can produce misleading interpretations of coefficients. First, we will demonstrate how cFLMM captures the instantaneous relationship between the photometry signal and within-trial licking behavior. We contrast the cFLMM approach with ncFLMM, showing that the interpretation of ncFLMM coefficients can be biased depending on the choice of behavioral summary (i.e. average lick rate) (Loewinger et al. (2025), Jeong et al. (2022)). Second, we will demonstrate how concurrent models can be deployed in experiments with variable trial length. We provide an example model for a foraging-like reward-seeking task where mice arrive at a reward zone at different trial timepoints (Machen et al.,2025) and evaluate the coefficient estimates against non-functional linear mixed model and ncFLMM baselines. Through these examples, we demonstrate that concurrent FLMMs can model a richer set of questions by allowing flexibility in controlling for changing conditions. This would be difficult to model with scalar covariates summarizing across within-trial timepoints.

Results and discussion

Concurrent FLMM modeling

Concurrent functional linear mixed modeling proceeds through the three broad steps of fitting univariate models, smoothing coefficients, and creating joint confidence intervals (Box 1), similar to the FLMM procedure described in Loewinger et al. (2025). However, unlike our previous

approach, concurrent models can take in experimental variables that vary across within-trial timepoints.

To describe this procedure, we can consider a hypothetical experiment investigating how the photometry signal changes based on a mouse's instantaneous velocity during the experiment, illustrated in Figure 1A-i. In the cFLMM, we model the association of photometry signal at each time point with the instantaneous mouse velocity at the same time point. More formally, let i index a mouse ID, j index trial number, and s indicate a specific time during trial j (i.e., the functional domain). We model the instantaneous photometry outcome for mouse i on trial j at trial timepoint s, $Y_{i,j}(s)$, as a function of the instantaneous mouse velocity $X_{i,j}(s)$, as shown in Fig 1A-ii. The notation (s) in the mouse velocity variable $X_{i,j}(s)$ indicates that its value can evolve across within-trial time-points, like the photometry signal, $Y_{i,j}(s)$. Our model allows the photometry–speed association to evolve across trial timepoints through the functional intercept $\beta_0(s)$, and the functional slope $\beta_1(s)$. The subject-specific random intercept $\gamma_{i,0}(s)$ and subject-specific random slope $\gamma_{i,1}(s)$ allow for the magnitude of these associations to vary across animal i and timepoints s. Finally, we denote random noise as $\epsilon_{i,j}(s)$, and formulate the model as:

$$Y_{i,j}(s) = \beta_0(s) + \gamma_{i,0}(s) + X_{i,j}(s)\left[\beta_1(s) + \gamma_{i,1}(s)\right] + \epsilon_{i,j}(s). \quad (1)$$

The outputs of this model are estimates $\hat{\beta}_0(s), \hat{\beta}_1(s)$ of the true fixed effect functional coefficient, $\beta_0(s)$ and $\beta_1(s)$, shown in Figure 1A-iii. We refer to these as *functional* regression coefficients because their values can vary over the course of trial timepoints, s. The estimated functional intercept $\hat{\beta}_0(s)$ can be interpreted as the average signal at s when the velocity at s is zero (i.e., $X_{i,j}(s) = 0$). The estimated functional slope $\hat{\beta}_1(s)$ is the average change in signal associated with a one unit change in velocity at s. For example, in Figure 1A-iii, $\hat{\beta}_1(1.2) = 0.61$, so a one-unit change in velocity is associated with a 0.61 unit increase in mean photometry signal at 1.2 seconds into the trial. This estimate is significantly higher than later in the trial (for example, $\hat{\beta}_1(3.0) = 0.35$), indicating that the association between signal and velocity becomes weaker as the trial progresses.

The model is fit to a dataset comprised of many trials for each of several animals, as shown in Figure 1B-i. While the fixed effects $\beta_0(s)$, $\beta_1(s)$ are pooled across all trials/animals, the random effects $\gamma_{i,0}(s)$, $\gamma_{i,1}(s)$ are perturbations to the fixed effects to represent animal-level differences, as illustrated in Figure 1B-ii. On the left plot of $\beta_1(s)$, the inset shows that $\hat{\beta}_1(3.2)$ is the estimated slope between photometry signal and velocity at $s = 3.2$ seconds. Likewise, on the right plot of $\hat{\beta}_1(s)+\widehat{\gamma_{1,2}}(s)$, the inset shows how the random effect allows the slope to differ between animals. Each animal's random effects are depicted in light gray, showing how animal-specific slopes are centered around the population fixed effect estimates. See Appendix 1 for more details on generating data for this demonstration.

Modeling behaviors that change over the trial

To illustrate how concurrent models capture effects of behaviors, we reanalyzed data from a previously published study on mesolimbic dopamine dynamics in learning (Jeong et al.,2022). In this experiment, head-affixed mice were provided with sucrose solution at random times with 100 sucrose deliveries per session. The authors of Jeong et al. (2022) were interested in modeling how the dopamine signal changes over the course of learning, i.e., modeling photometry signal as a function of session, trial, and inter-reward interval. Variable reward timing can complicate the analysis, as the signal is aligned to when the mouse licks the sucrose delivery mechanism rather than the moment when the sucrose is available. Furthermore, although mice were more prone to licking after reward delivery, each trial contained random unrewarded licking behavior before and immediately after delivery, as shown in Figure 2A-i. Previously, Jeong et al. (2022) modeled the signal, shown in Figure 2A-ii, by averaging the photometry response in a predefined period after the first post-reward lick. In Loewinger et al. (2025), we modeled the entire functional outcome of photometry. We aligned trials to the first lick, and estimated the

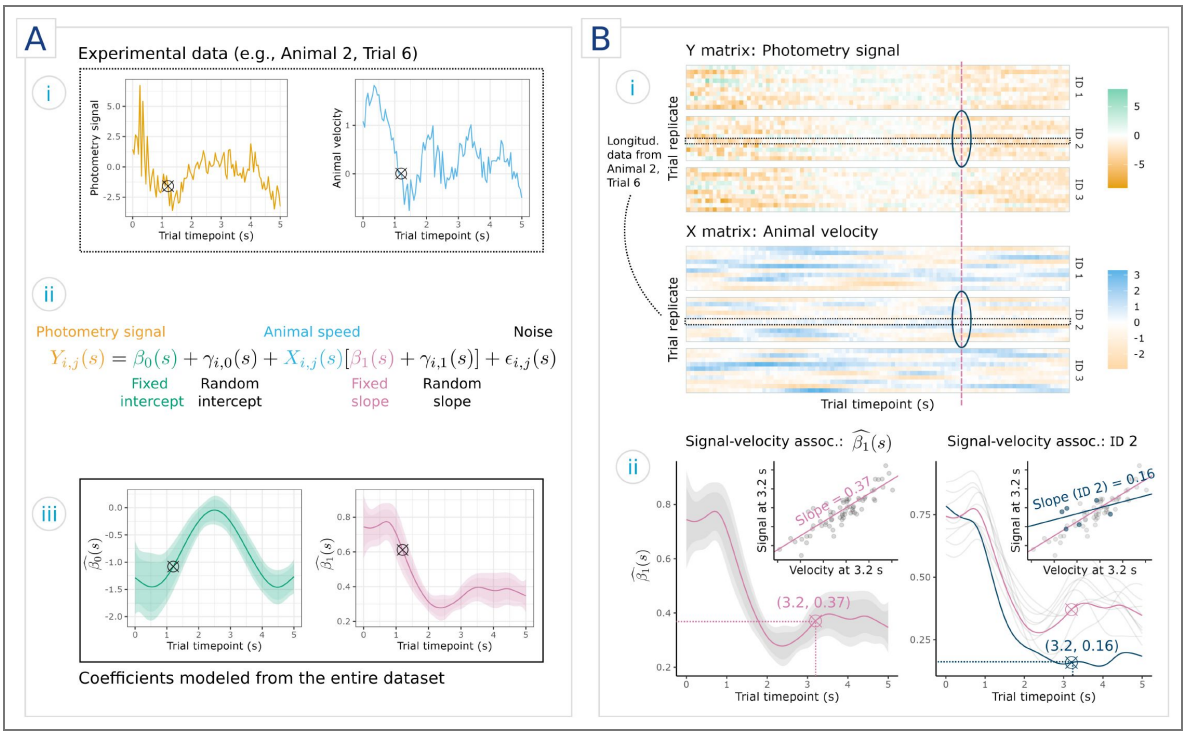

Figure 1. Visualization of an example concurrent functional linear mixed model on synthetic data.

A) **A-i**) Functional outcomes (photometry signal) and inputs (animal velocity) over one trial, **A-ii**) labeled model equation for the time point marked with cross-hairs in (i) and (iii), **A-iii**) output functional fixed coefficients $\beta_0(s)$ and $\beta_1(s)$. **B**) Example experimental data and interpretation of effects, including the **B-i**) heat maps of the photometry dataset and speed dataset (groups are subjects *i*, rows are trials *j*, and columns are time points *s*), and **B-ii**) fixed effects at a given timepoint (left) and random effects at the same point (right).

association between the inter-reward interval and photometry signal. In contrast, here we centered the signal to reward delivery and then estimated the association between moment-by-moment lick behavior and the photometry signal.

Photometry signal as a function of intermittent licking behavior

To align with previous analyses in Loewinger et al. (2025) and Jeong et al. (2022)'s interest in longitudinal effects on photometry signal, we incorporated trial-specific covariates for trial number and session, modeling these as increasing numerical values rather than identical categorical variables. Modeling the experiment with a concurrent FLMM provides several advantages over the previous models. The time-dependence of the relationship between signal and licking behavior can be visualized without incorporating an additional covariate of reward-lick latency, which summarizes the trial-level lick timeseries. Unlike previous analyses, the concurrent model does not require discarding trials where the first lick occurs too quickly after the reward delivery. The concurrent model can directly estimate that the dopamine signal contribution of licking behavior ($\beta_1(s)$) is zero prior to and immediately after reward delivery, rises 0.2 seconds after the reward is delivered, and peaks at around 0.3 seconds after reward delivery (Fig. 2B-i). We also include the fixed effects for trial and session in Appendix 3.

Comparison to non-concurrent models

We conducted a sensitivity analysis to assess how fitting a non-concurrent FLMM model would influence the coefficients and interpretation. We summarized licking behavior as a trial-specific scalar covariate, calculated as the average lick rate in a defined reward period T after sucrose delivery. We compared coefficient estimates for models of T = 0.5, 1.0, 2.0 seconds (Fig. 2Bii-iv).

While the trends of the fixed coefficients are similar to the concurrent model, the peak of the estimated effect is dependent on the choice of L. As reward periods are longer, the estimated peak occurs later. This trend may be due to different underlying lick dynamics resulting in the same summary statistic, leading to a flattening of coefficient estimates along the region used to summarize the behavioral data.

Furthermore,the point estimates of the ncFLMM fixed effect coefficients are negative later in the trial, unlike the concurrent model. However, because the underlying summary covariate analyzed in the ncFLMMs ignores these regions entirely, the modeled coefficients outside of the period L may be deceptive, as behavioral data in this region do not contribute to the average lick rate summary statistic. Although the point estimates imply that increased lick rates later in the trial are associated with lower expected signal outcome, it may be possible that the expected signal outcome is positive, but the lick rate is lower outside of L, causing the apparent negative effect. Although ncFLMM avoids the need to summarize photometry signal over the trial, the resulting models may still be biased due to transforming functional covariates into trial-specific scalars.

Modeling behaviors in trials of varying lengths

In some experimental designs, trial length differs due to behavior or experimental conditions. Concurrent FLMMs can be applied to avoid issues with devising a fair summarization statistic of the photometry signal or behavior. To demonstrate this, we carried out an example cFLMM analysis in an experiment where mice receive rewards at inconsistent times. Mice were trained to wait in a trigger zone, run through a corridor, then receive a food reward in the reward delivery zone. Investigators were interested in testing whether the mean photometry signal changed based on the speed at which mice through the corridor, or the reward delivered (either a strawberry milkshake solution (SMS) or water. Machen et al. (2025) tests more reward conditions, such as a non-caloric but sweet reward, though these are excluded for brevity. Within this setup, a natural way to define trials would be to summarize the signal over the period when the mouse is in the reward zone. However, this approach produces trials of different lengths, introducing bias depending on the choice of summary statistic.

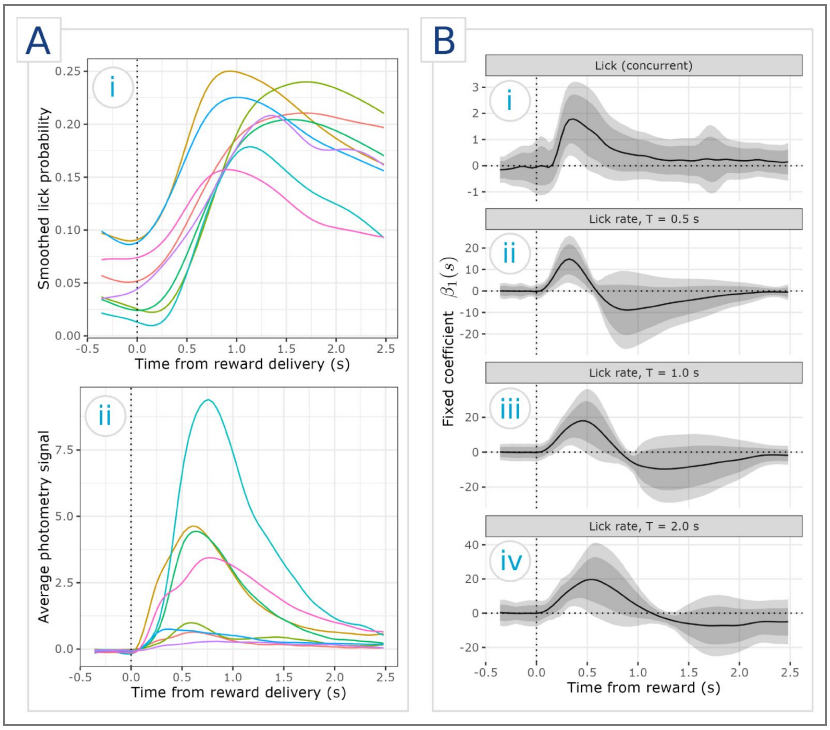

Figure 2. Fitted coefficients for concurrent and non-concurrent models of the expected signal with respect to licking behavior in mice randomly delivered sucrose solution.

A) Features of the experimental data. **A-i**) The distribution of licking behaviors, averaged within mice and smoothed for readability, with one curve per mouse. **A-ii**) Photometry signal, averaged within mice. **B**) Estimates of the functional fixed coefficient $\beta_1(s)$ corresponding to different choices of FLMM and behavioral covariate. **B-i**) Concurrent model with an instantaneous functional covariate tracking licking behavior. **B-ii-iv**) Non-concurrent models with a trial-specific scalar covariate for the lick rate **ii**) 0.5 seconds after reward delivery, **iii**) 1.0 seconds after reward delivery, and **iv**) 2.0 seconds after reward delivery. Fixed effect estimates for trial and session can be found in Appendix 3.

Baseline 1: Non-functional linear mixed model

We demonstrated that summarizing functional data over time can be unreliable in this setup by producing two non-functional linear mixed models (LMMs) with different approaches to summarizing experimental variables (Eqn. 6). As before, let s indicate the trial timepoint, i index the animal ID, and j index the trial number. Let $S_{i,j,R}$ be the set of timepoints where mouse i is in the reward zone in trial j. We compared models where the summary statistic was the average $\bar{Y}_{i,j} = \frac{1}{\|S_{i,j,R}\|}\sum_{S_{i,j,R}} Y_{i,j}(s)$ or the sum $\check{Y}_{i,j} = \sum_{S_{i,j,R}} Y_{i,j}(s)$ of photometry signals over the reward zone. For both choices, we found a strongly significant signal increase associated with the SMS reward ($p < 0.0001$). For $\bar{Y}_{i,j}$, we found that the point estimates for latency and the interaction of the SMS reward and latency were both positive (Fig. 3A-i). Conversely, with the sum $\check{Y}_{i,j}$, these point estimates were both negative (Fig. 3A-ii). This difference suggests that a sum over the period may overestimate the importance of arriving at the reward early, while an average signal penalizes an early arrival. In practice, choosing a summary may require prior knowledge of signal dynamics during the reward period, which may introduce bias in interpretation.

Baseline 2: Non-concurrent FLMM interaction model

Although a non-concurrent FLMM can capture the functional associations between the signal and behavioral data, the model produces coefficient estimates that could lead to misleading scientific conclusions. Because the non-concurrent model cannot use the moment-by-moment mouse location data, we summarized the behavior of each trial as a single scalar value of latency, i.e., how long it took for a mouse to reach the reward region from trial onset (Fig 3B) (Eqn. 7). Furthermore, for ease of interpretation, we centered trial latency. In the non-concurrent model, there are significant signal effects associated with the SMS reward, latency, and their interaction (Fig 3B). On trials with average latency, there is a significant increase in signal for mice receiving SMS (Fig 3B-ii) versus receiving the water baseline (Fig 3B-i) between 2 and 8 seconds into the trial. Increasing latency is associated with a negative effect on signal starting at trial start (zero seconds), reaching a minimum at around three seconds into the trial, and returning to zero at around 6 seconds into the trial (Fig 3B-iii). The shape of the fixed coefficient estimate for the interaction of SMS reward and latency is similar, though becomes slightly positive near the end of the trial (Fig 3B-iv).

cFLMM incorporating trial lengths as a functional interaction

For our concurrent model, we incorporated a binary functional covariate indicating whether the mouse had received the reward. We modeled an interaction between the reward indicator and the reward type (SMS or water) (Eqn. 8 in Variable trial length analysis). Unlike non-concurrent FLMMs, there is no expected difference in signal when a mouse has not yet received a reward, regardless of reward type (water or SMS) (Fig 3C-i, C-ii). However, expected signal change is positive early in the trial when mice receive a baseline reward (Fig 3C-iii), with an additional positive effect when the reward is SMS (Fig 3C-iv).

Interpreting non-concurrent FLMM vs. cFLMM coefficients

The concurrent model coefficients are more easily interpretable because the model separates the experiment into the relevant, discrete events. The first two fixed coefficients, for example, correspond to the expected signal for mice in a water trial that have not received a reward (Fig 3C-i) and mice in a SMS trial that have not received a reward (Fig 3C-ii). For both conditions, the estimated coefficients were not significantly different from zero and confirmed the experimental assumption that mice have no knowledge of what trial they are in before they receive a reward. The last two fixed coefficients, corresponding to signal for baseline reward (Fig 3C-iii) and the difference of SMS reward and baseline reward (Fig 3C-iv), separated the signal response attributable to receiving a reward in general versus receiving a desirable reward. Furthermore, the time dependence of all of these effects is captured by the functional nature of the coefficients and underlying covariates.

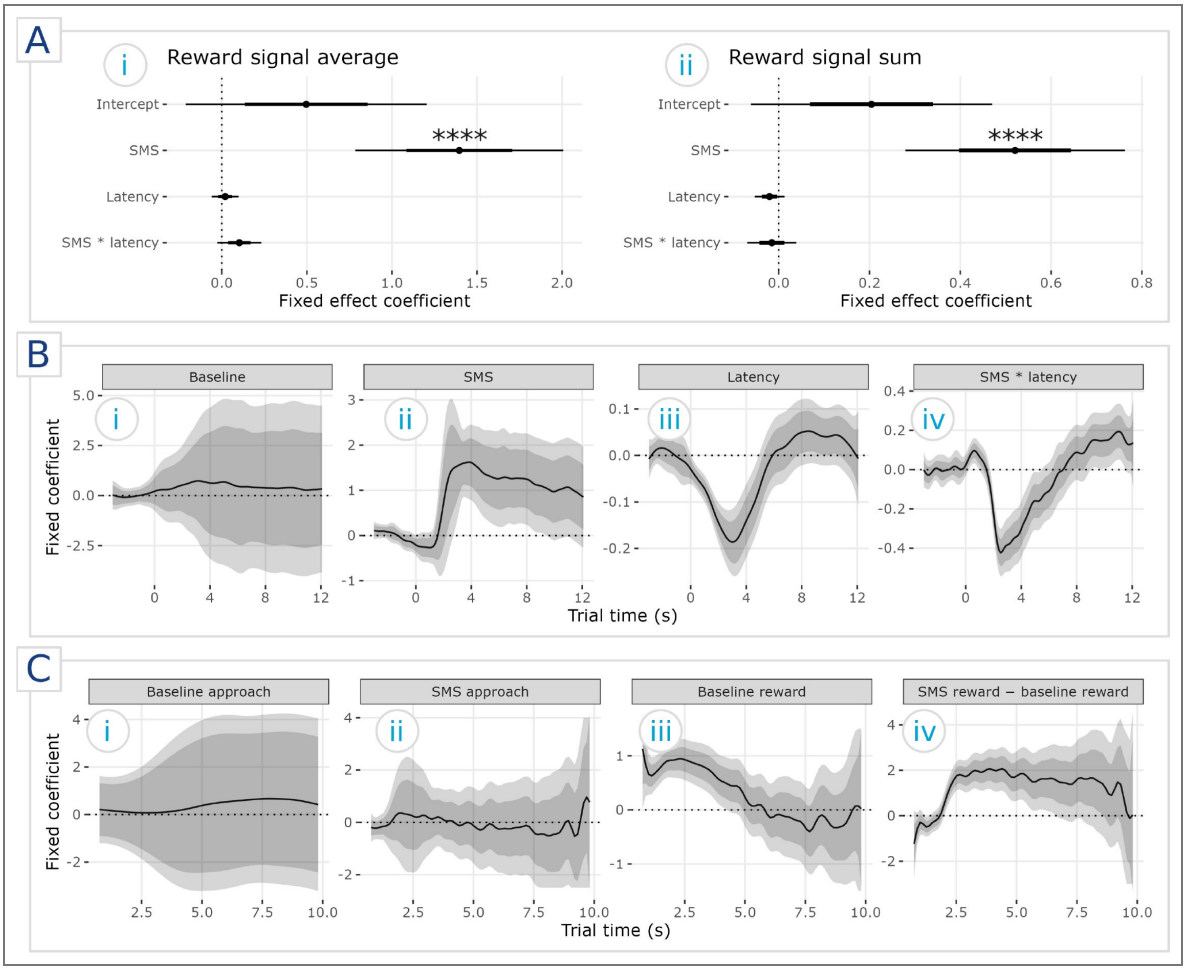

Figure 3. Comparisons of coefficient estimates for an experiment where mice receive different rewards at variable times.

A Fixed coefficients in a non-functional linear mixed model fit to **A-i** the average of the photometry signal in the reward period or **A-ii** the sum, with $****$: $p \leq 0.0001$. **B** Functional fixed coefficients in a non-concurrent functional linear mixed model, corresponding to **B-i**) the intercept, i.e., the expected signal when latency is average and the mouse is given water; **B-ii**) the expected signal when latency is average and the mouse is given SMS; **B-iii**) the slope of mean signal change with respect to (w.r.t.) change in latency; and **B-iv**) the slope of mean signal change w.r.t. change in latency when the mouse is rewarded with SMS. C Functional fixed coefficients in a concurrent functional linear mixed model, corresponding to **C-i**) the intercept, i.e., the expected change in signal when a mouse in the baseline water condition has not yet received a reward; **C-ii**) unrewarded SMS, i.e., the expected change in signal when a mouse in the SMS condition has not yet received a reward; **C-iii**) baseline reward change, i.e., the expected difference in signal between a mouse receiving water and not receiving water; and **C-iv**) SMS reward change minus baseline reward change, i.e., the expected difference between receiving SMS and not receiving SMS and the value described in **A-iii**.

Within the non-concurrent FLMM, the instantaneous interpretation of the coefficients is less pertinent to the question of identifying the association between average signal and behavior. For example, the ncFLMM predicted no association when in a trial where water is the reward (Fig 3B-i) and a positive association in a trial where SMS is the reward (Fig 3B-ii). However, we know from analyzing the data that average latency across all mice and trials is also around 3 seconds. Thus, the observed peak in signal at around 3 seconds has an ambiguous interpretation, as it could be attributed to either receiving the SMS reward at that time or simply finishing the task.

Incorporating the estimated latency coefficients further complicates the interpretation of the ncFLMM. The dip in the estimated coefficients at around 3 seconds does not necessarily mean that mice with a slower-than-average latency will have a lower photometry response when they reach the reward. It could reflect that, in general, rewards increase the photometry signal magnitude and the slow mice have not yet reached the reward zone (Fig 3B-iii). The shape of the coefficient curve for the interaction `SMS * latency` also shows a dip, which seems to contradict the concurrent model's estimate that SMS elicits a larger mean signal than water upon reward. However, the coefficients cannot be interpreted as effects associated with reward time, but only the effects at a specific trial time. The shape of the `SMS * latency` interaction functional coefficient can be explained as a correction for the strongly positive `SMS` main effect functional coefficient for slower-than-average mice. For example, a mouse receiving an SMS reward running a trial with a latency of 8 seconds does not exhibit, on average, a larger signal than on water trials at the trial timepoint of 4 seconds (doing so would imply prescience of the reward type). Thus, the negative `SMS * latency` coefficient estimate indicates that signal should be lower than what would be suggested by the `SMS` functional coefficient estimate at 4 seconds, as the `SMS` coefficient estimate reflects the estimated signal for mice running at an average latency.

Potential drawbacks of the functional covariate approach

For this particular problem, the non-concurrent model can model a larger functional domain than its concurrent counterpart. The functional coefficients for FLMMs are obtained by fitting individual linear mixed models at each point on the functional domain. When estimating the coefficients for a concurrent FLMM, each point must produce an identifiable model. This condition may be violated if a covariate has very low variance across every observation (e.g., mice never arrive at the reward zone early in the trial). Because all mice are approaching the reward at the start of trial and all mice are rewarded by the end of the trial, the concurrent FLMM cannot fit the extreme ends of the trial time frame. Here, this limitation is not relevant because there are likely no significant differences in mice when they are all experiencing the same condition. In this experiment in particular, mice are unaware of the reward they will receive when the experiment begins, and trials are unlikely to be meaningfully different within this time period.

The concurrent model also groups together all mice in the reward zone, which can suppress effects later in the trial. The indicator functional covariate is insensitive to how long ago a mouse has been reward, so a mouse that has just been rewarded and a mouse that has been rewarded much earlier in the trial are considered identical. Thus, the observed trend toward zero in the functional fixed effect estimates for the water reward and SMS reward may not indicate that mice have a lower photometry outcome response if they run slower (Figs. 3C-iii, -iv). Instead, the decrease may be partially attributed to more mice waiting in the reward period, diluting the observed signal outcome of newly-rewarded mice.

Verification of method performance in simulations

Our concurrent FLMM approach produces both a *pointwise* and a *joint* confidence band for each coefficient time series. We produce the pointwise confidence band by estimating the variance of the fixed effects at each point and constructing appropriate 95% confidence intervals at each smoothed fixed effect estimate. The joint confidence band accounts for autocorrelation of signal values and produces a confidence band that corresponds to a hypothesis test across all timepoints simultaneously. To evaluate both the pointwise and joint confidence interval coverage of the concurrent FLMM models, we simulated data from a known model in a variety of realistic settings of dataset size and noise. We calculated pointwise coverage by finding the empirical coverage

probability at each point and then averaging across the domain. In contrast, we assessed joint coverage by finding the empirical coverage probability of the confidence band, i.e., the probability that the entirety of the true fixed effects function lies within the estimated joint confidence band.

We simulated data generated from the following model

$$Y_{i,j}(s) = \beta_0(s) + \gamma_{i,0}(s) + X_{i,j}(s)\beta_1(s) + \epsilon_{i,j}(s), \quad (2)$$

which contains a fixed intercept $\beta_0(s)$, fixed slope $\beta_1(s)$, and random intercept $\gamma_0(s)$. Within these simulations, we assumed that noise can arise from between-animal heterogeneity, e.g., individual differences affecting the magnitude of association between velocity and photometry signal. Furthermore, we also incorporated random measurement noise uncorrelated with experimental variables. These noise components were defined as 1) the signal-noise ratio of fixed effects to random effects SNR_B, i.e., effect heterogeneity that arises from animal-level differences, and 2) the signal-noise ratio of true underlying values to random Gaussian noise SNR_σ, i.e., the $\epsilon_{i,j}(s)$ term in Equation 2. We also refer to these components as measurement noise and between subject variability, respectively. We performed 200 replicates of 5, 10, ..., 45, 50 subjects (simulated animals) with 100 trials each. Specific implementation details and examples of noisy data are included in Appendix 2.

We found that coverage generally asymptotes at ≥ 10 subjects for all noise conditions (Fig 4), though the value of the asymptotic coverage is dependent on the specific levels of noise. The signal-noise ratio of fixed effects to random effects (SNR_B) shows a more pronounced effect on coverage than the relative importance of Gaussian noise (SNR_σ) for both joint and pointwise coverage. Joint coverage tends to be overconfident when $\text{SNR}_B = 1$, close to theoretical 95% coverage when $\text{SNR}_B = 1/2$, and conservative when $\text{SNR}_B = 1/3$ and Gaussian noise is low (Fig 4A). Pointwise coverage tends to be conservative in all tested conditions except for $\text{SNR}_B = 1$ (Fig 4B).

The simulation results suggest that relatively high levels of subject-specific effects impede coverage more than high levels of random measurement noise. Even in settings where the standard deviation of Gaussian noise is equal to that of the underlying signal ($\text{SNR}_\sigma = 1$, leftmost column in Fig 4), joint coverage achieves 95% for 15 subjects when $\text{SNR}_B = 1/2$ and 5 subjects when $\text{SNR}_B = 1/3$. However, when $\text{SNR}_B = 1$ (topmost rows in A, B of Fig 4), joint coverage peaks at around 90% regardless of the number of subjects or level of SNR_σ. Barring high levels of between-subject variability, coverage is likely valid, albeit conservative.

Materials and methods

Concurrent FLMM estimation

General form of cFLMMs

Let p be the number of fixed effects, q be the number of random effects, i be the animal ID, j be the trial number, and l be the session number. We describe the concurrent functional linear mixed model of $Y_{i,j,l}(s)$, or the photometry signal at timepoint s for animal i, trial j, and session l), with the generic mean model

$$\mathbb{E}[Y_{i,j,l}(s)|\mathbf{X}_{i,j,l}(s), \mathbf{Z}_{i,j,l}(s), \boldsymbol{\gamma}_{i,j,l}(s)] = \mathbf{X}^T_{i,j,l}(s)\boldsymbol{\beta}(s) + \mathbf{Z}^T_{i,j,l}(s)\boldsymbol{\gamma}_{i,j,l}(s)$$

where subscripts reflect whether variables are subject-, trial-, or session-specific. In this formulation, $\mathbf{X}_{i,j,l}(s)$ is the p×1 column vector of covariates for fixed effects, $\mathbf{Z}_{i,j,l}(s)$ is the q ×1 column vector of covariates for random effects, $\boldsymbol{\gamma}_{i,j,l}(s)$ is the q × 1 column vector of random effects, and $\boldsymbol{\beta}(s)$ is the p × 1 column vector of fixed effects. We assume a Gaussian distribution for the conditional likelihood $Y_{i,j,l}(s)\,|\,\mathbf{X}_{i,j,l}(s), \mathbf{Z}_{i,j,l}(s), \boldsymbol{\gamma}_{i,j,l}(s)$.

Throughout this paper, we write models as expressions with the explicit form

$$Y_{i,j,l}(s) = \mathbf{X}_{i,j,l}(s)\boldsymbol{\beta}(s) + \mathbf{Z}_{i,j,l}(s)\boldsymbol{\gamma}_{i,j,l}(s) + \epsilon_{i,j,l}(s)$$

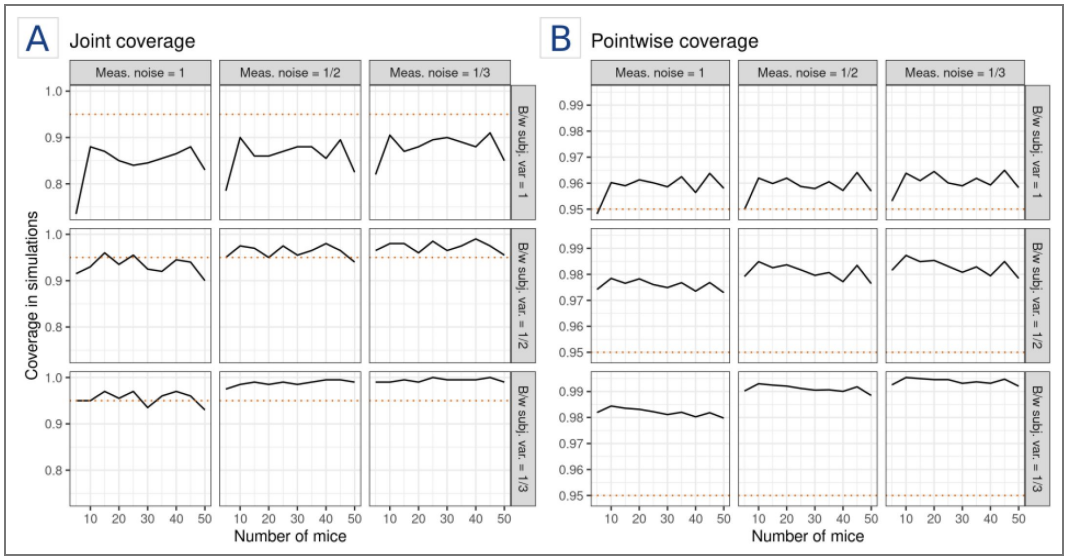

Figure 4. Nominal coverage achieved in simulations, reported as A) joint coverage and B) pointwise coverage for different values of measurement noise (meas. noise) and between subject variability (b/w subj. var.).

Simulations were performed on 200 replicates of each condition. The horizontal red dotted line indicates the theoretical 95% coverage mark.

where we assume random effects $\boldsymbol{\gamma}_i(s) \in \mathbb{R}^q$ and noise terms $\boldsymbol{\epsilon}(s) \in \mathbb{R}^1$ are mutually independent and Normally distributed. Estimates for random effects $\boldsymbol{\beta}(s)$ and fixed effects $\boldsymbol{\gamma}_i(s)$ are correlated across the functional domain. When describing cFLMM models, we replace the general vector notation $\mathbf{X}_{i,j,l}$ with individual covariate terms and descriptive names (e.g., $\texttt{Lick}_{i,j,l}(s)$).

Methodological contributions to joint confidence interval estimation

We provide a high-level overview of the methodological details of the concurrent FLMM here and include a more detailed description in Appendix 3 of Loewinger et al. (2025). The main methodological contribution required for this approach is an extension of a method of moments covariance estimator needed to compute $\text{Var}(\hat{\boldsymbol{\beta}})$ and calculate 95% confidence intervals. Briefly, after fitting pointwise linear mixed models, we obtain estimates of the fixed effects $\hat{\boldsymbol{\beta}}(s)$ at each within-trial timepoint s. As in Loewinger et al. (2025); Cui et al. (2022), the covariance between fixed effects estimates can be described as

$$\text{Cov}\left(\hat{\boldsymbol{\beta}}(s_1), \hat{\boldsymbol{\beta}}(s_2)\right) = \left[\mathbf{X}^T(s_1)\mathbf{V}^{-1}(s_1)\mathbf{X}(s_1)\right]^{-1}\mathbf{X}^T(s_1)\mathbf{V}^{-1}(s_1)\mathbf{W}(s_1, s_2)\mathbf{V}^{-1}(s_2)\mathbf{X}(s_2)\left[\mathbf{X}^T(s_2)\mathbf{V}^{-1}(s_2)\mathbf{X}(s_2)\right]^{-1}, \tag{3}$$

where we define

- $\mathbf{X}(s)$: the design matrix for the fixed coefficients at point s,
- $\mathbf{Z}(s)$: the design matrix for the random coefficients at point s,
- $\mathbf{V}(s) = \mathbf{Z}(s)\mathbf{H}(s)\mathbf{Z}(s)^T + \mathbf{R}(s)$, where $\mathbf{H}(s)$ and $\mathbf{R}(s)$ are the covariance matrices of $\boldsymbol{\gamma}(s)$ and $\boldsymbol{\epsilon}(s)$, respectively and estimates $\hat{\mathbf{H}}(s)$ and $\hat{\mathbf{R}}(s)$ can both be obtained from the first step,
- $\mathbf{W}(s_1, s_2) = \mathbf{Z}(s)\mathbf{G}(s_1, s_2)\mathbf{Z}^T(s)$, where $\mathbf{G}$ is the covariance matrix of random effects and $\mathbf{G}(s_1, s_2) = \text{Cov}(\boldsymbol{\gamma}(s_1), \boldsymbol{\gamma}(s_2))$, where $\boldsymbol{\gamma}(s)$ is a one-dimensional vector concatenating the random effects for all subjects at point s.

In contrast with non-concurrent FLMMs, covariance estimation for cFLMMs incorporates unique $\mathbf{Z}(s)$ and $\mathbf{X}(s)$ values at each point on the functional domain. The number of calculations required to obtain an estimate grows combinatorially with respect to the size of the functional domain L, the number of random effects, and the number of fixed effects, resulting in a highly memory-intensive procedure. This step can become computationally infeasible for even moderately-sized datasets if carried out naively. A major methodological contribution of this work was deriving a computationally efficient procedure, described in Appendix 4.

R package for cFLMM fitting

We incorporated cFLMM fitting into our existing package `fastFMM`, published on GitHub `awqx/fastFMM`. Concurrent models can be fit with the same notation as ncFLMMs by adding the argument `concurrent = TRUE` to the function `fastFMM::fui`. The following sections will provide examples of the code needed to fit both ncFLMMs and cFLMMs with `fastFMM`.

Reanalysis of photometry measures of dopaminergic neurons

When applying concurrent FLMMs to time-varying behaviors, we re-analyzed data from Experiment 3 published in Jeong et al. (2022), as described in Modeling behaviors that change over the trial. We briefly explain the experimental design before describing the model that we applied. The original authors of Jeong et al. (2022) presented head-affixed mice with sucrose solution, with delivery times distributed exponentially with a mean of 12 seconds and 100 sucrose rewards within a single session. In our analysis, we defined trials as a window 0.4 seconds before and 2.5 seconds after reward delivery, with overlapping trials discarded. We specified the concurrent model as:

$$Y_{i,j,l}(s) = \beta_0(s) + \gamma_{i,0}(s) + [\beta_1(s) + \gamma_{i,1}(s)]\texttt{Lick}_{i,j,l}(s) + \beta_2(s)\texttt{SN}_{i,j,l} + \beta_3(s)\texttt{TN}_{i,j,l} + \epsilon_{i,j,l}(s), \tag{4}$$

where i indexes the mouse ID, j indexes the trial number, and l indexes the session number. $Y_{i,j,l}(s)$ is the observed signal and $\epsilon_{i,j,l}(s)$ is the observed noise at s for subject i, trial j, and session l. We included the covariates

- $\texttt{Lick}_{i,j,l}(s)$: the functional covariate of licking behavior, where $\texttt{Lick}(s) = 1$ when mouse i on trial j of session l is licking at time s and $\texttt{Lick}(s) = 0$ otherwise,
- $\texttt{SN}_{i,j,l}$: the shifted and scaled session number, and
- $\texttt{TN}_{i,j,l}$ the shifted and scaled trial number.

Regressors $\texttt{SN}$, $\texttt{TN}$ are included because there may be temporal effects within a session (e.g. satiation), or between sessions (e.g. practice). We transformed $\texttt{SN}$, $\texttt{TN}$, by subtracting one and dividing by the maximum session number and trial number, respectively. This modification aids interpretation by setting the first session at zero and the max session as one. Shifting and scaling does changes the magnitude of estimated coefficients but not the shape. We recommend scaling when covariates have very different magnitudes. E.g., here, trials range from 1 to 100 while licks range from 0 to 1.

We included the random effects

- $\gamma_{i,0}(s)$: the random intercept for mouse i at time s. This is interpreted as the average photometry signal at s of mouse i on trials when when $\texttt{Lick}_{i,j,l}(s) = \texttt{SN}_{i,j,l} = \texttt{TN}_{i,j,l} = 0$, and
- $\gamma_{i,1}(s)$ the random slope associated with the licking behavior for mouse i at time s, and the fixed coefficients

- $\beta_0(s)$: the intercept when $\texttt{Lick}_{i,j,l}(s) = \texttt{SN}_{i,j,l} = \texttt{TN}_{i,j,l} = 0$, i.e., the mean signal at s on the first trial and first session when the mouse is not licking,
- $\beta_1(s)$: the mean effect on the signal associated with licking behavior at s,
- $\beta_2(s)$: the mean effect on the signal associated with the session number $\texttt{SN}_{i,j,l}$ at time s, and
- $\beta_3(s)$: the mean effect on the signal associated with the trial number $\texttt{TN}_{i,j,l}$ at time s.

We fit the concurrent model with the R code

```
fastFMM::fui(
formula = photometry ~ session + trial + lick + (1 + lick | id),
data = data,
concurrent = TRUE
)
```

We fit the non-concurrent model

$$Y_{i,j,l}(s) = \beta_0(s) + \gamma_{i,0}(s) + [\beta_1(s) + \gamma_{i,1}(s)]\texttt{LR}_{i,j,l} + \beta_2(s)\texttt{SN}_{i,j,l} + \beta_3(s)\texttt{TN}_{i,j,l} + \epsilon_{i,j,l}(s), \quad (5)$$

where we replaced $\texttt{Lick}_{i,j,l}(s)$ with the scalar $\texttt{LR}_{i,j,l} = \frac{1}{|T|}\sum_{s\in T}\texttt{Lick}_{i,j,l}(s)$, corresponding to the lick rate in the time region T after the reward delivery. To calculate $|T|$, we multiplied the number of seconds in T (either 0.5, 1.0, or 2.0) by the measurement frequency of 25 Hz. We fit the non-concurrent model with the R code

```
fastFMM::fui(
formula = photometry ~ session + trial + LR + (1 + LR | id),
data = data,
concurrent = FALSE
)
```

where $\texttt{LR}$ varied depending on the specified time period T.

Variable trial length analysis

In Modeling behaviors in trials of varying lengths, we reanalyzed data from a foraging-like reward-seeking task, where mice run through a corridor and enter a reward zone at different times (Machen et al.,2025). Throughout this section, let i index the mouse and j index the trial. The non-functional linear mixed model contains no functional terms, and we defined it as

$$Y_{i,j} = \beta_0 + \gamma_{i,0} + (\beta_1 + \gamma_{i,1})\texttt{SMS}_{i,j} + \beta_2\texttt{Lat}_{i,j,2} + \beta_3\texttt{SMS}_{i,j}\texttt{Lat}_{i,j} + \epsilon_{i,j}(s), \quad (6)$$

where the trial-specific scalar outcome $Y_{i,j}$ is either $\overline{Y}_{i,j}$ or $\check{Y}_{i,j}$, which denotes the average or the sum of the signal over the reward period, respectively. We defined the covariates

- $\texttt{SMS}_{i,j}$: the trial outcome, where $\texttt{SMS}_{i,j} = 1$ for a trial with strawberry milkshake (SMS) and $\texttt{SMS}_{i,j} = 0$ for water, and
- $\texttt{Lat}_{i,j}$: the latency, in seconds, until mouse i in trial j received the food reward.

For ease of interpretation, we centered the latency values, so $\texttt{Lat}_{i,j,2}$ is the difference between the latency in that trial and the average latency across all trials. For example, $\texttt{Lat}_{i,j} < 0$ when mouse i in trial j ran the corridor faster than average and $\texttt{Lat}_{i,j} > 0$ when mouse i in trial j ran slower than average. The random effects are

- $\gamma_{i,0}$: the random intercept for mouse i, interpreted as the average photometry signal of mouse i on trials with water reward and average latency, and
- $\gamma_{i,1}$ the random slope for mouse i, interpreted as the subject-specific association between signal and the SMS reward for mouse i on average latency,

and the fixed effect coefficients are

- β_0: the intercept when $\texttt{SMS}_{i,j} = \texttt{Lat}_{i,j} = 0$, i.e., the mean signal on water trials when a mouse responds with an average latency,
- β_1: the mean difference in signals between SMS and water trials when a mouse responds with an average latency,
- β_2: the change in mean signal associated with a one second increase in latency on water trials, and
- β_3: the difference $A - B$ between A) the change in mean signal associated with a one second increase in latency on SMS trials and B) β_2.

We fit the two linear mixed models with the R package `nlme` (Pinheiro et al.,2025) with the code

```
lme_avg <- nlme::lme(
fixed = photo_avg ~ SMS * latency,
random = ~ outcome | id,
data = data
)
lme_sum <- nlme::lme(
fixed = photo_sum ~ SMS * latency,
random = ~ SMS | id,
data = dat
)
```

where the interaction term implicitly includes the individual terms `SMS` and `latency` in the model. Our non-concurrent FLMM treated the entire trial photometry signal as a functional outcome $Y_{i,j}(s)$. We specified the ncFLMM model as

$$Y_{i,j}(s) = \beta_0(s) + \gamma_{i,0}(s) + [\beta_1(s) + \gamma_{i,1}(s)]\texttt{SMS}_{i,j} + \beta_2(s)\texttt{Lat}_{i,j} + \beta_3(s)\texttt{SMS}_{i,j}\texttt{Lat}_{i,j} + \epsilon_{i,j}(s). \quad (7)$$

The interpretations of the random and fixed effects are analogous to the non-functional linear mixed model. However, in the functional setting, the coefficients correspond to associations between the signal at time s and the covariates. We fit the ncFLMM with the code

```
fastFMM::fui(
photometry ~ SMS * latency + (SMS | id),
data = data,
concurrent = FALSE
)
```

where the interaction term implicitly includes the individual terms `SMS` and `latency` in the model.

The cFLMM model incorporated the functional covariate of $\texttt{RZ}_{i,j}(s)$ (reward zone) instead of the scalar covariate $\texttt{Lat}_{i,j}$. We specified the cFLMM model as

$$Y_{i,j}(s) = \beta_0(s) + \gamma_{i,0}(s) + [\beta_1(s) + \gamma_{i,1}(s)]\mathrm{SMS}_{i,j} + \beta_2(s)\mathrm{RZ}_{i,j}(s) + \beta_3(s)\mathrm{SMS}_{i,j}\mathrm{RZ}_{i,j}(s) + \epsilon_{i,j}(s), \quad (8)$$

where $\mathrm{RZ}_{i,j}(s) = 0$ if mouse i in trial j was in the corridor approaching the reward zone at time s, and $\mathrm{RZ}_{i,j}(s) = 1$ if mouse was in the reward zone at time s. The random effects are interpreted as

- $\gamma_{i,0}(s)$: the random intercept for mouse i, or the subject-specific average perturbation of $\beta_0(s)$ such that $\beta_0(s) + \gamma_{i,0}(s)$ is the average signal for mouse i on water trials at time s when the reward has not yet been received, and
- $\gamma_{i,1}(s)$: the random slope for mouse i, or the subject-specific average perturbation of $\beta_1(s)$ such that $\beta_1(s) + \gamma_{i,1}(s)$ is the average photometry signal change associated with being in an SMS trial for mouse i at time s when the reward has not yet been received,

and the functional fixed coefficients are interpreted as

- $\beta_0(s)$: the mean signal on a water trial at a timepoint s when the reward has not yet been received, i.e., when $\mathrm{RZ}_{i,j}(s) = \mathrm{SMS}_{i,j} = 0$,
- $\beta_1(s)$: the mean difference in signal between SMS and water trials at a timepoint s when the reward has not yet been received,
- $\beta_2(s)$: the average difference between approach and reward in water trials at time s, and
- $\beta_3(s)$: the difference in differences $A - B$ between A) the average signal difference between approach and reward on SMS trials, and B) the average difference in signal values between approach and reward on water trials (i.e., β_2), at trial timepoint s.

Here, $\beta_3(s) = 0$ when the association between reward type and the photometry signal does not change depending on the type of reward given. Conversely, $\beta_3(s) > 0$ if, compared to water trials, SMS trials are linked with a greater change in mean signal between being in the reward zone versus the corridor at s. That is, $\beta_3(s)$ captures how the photometry signal is changed by a dynamic interaction between the type of reward and the behavior of the mouse. We fit the cFLMM with the code

```
fastFMM::fui(
photometry ~ SMS * RZ + (SMS | id),
data = data,
concurrent = TRUE
)
```

where the interaction term implicitly includes the individual main effect terms `SMS` and `RZ` in the model.

Acknowledgements

First, we thank Dr. Sofia Beas, the corresponding author and principal investigator of "The encoding of interoceptive-based predictions by the paraventricular nucleus of the thalamus D2R+ neurons", for sharing experimental data and helping us interpret the results. We also thank Drs. Vijay Namboodiri and Huijeong Jeong, the corresponding authors of "Mesolimbic dopamine release conveys causal associations," who generously shared their data and provided support for our previous publication, "A statistical framework for analysis of trial-level temporal dynamics in fiber photometry experiments".

Simulation results in this study utilized the computational resources of the NIH HPC Biowulf cluster (*https://hpc.nih.gov*). This research was supported in part by the Intramural Research Program of the National Institutes of Health (NIH) (ZIC MH002968). The contributions of the NIH author(s) were made as part of their official duties as NIH federal employees, are in compliance with agency policy requirements, and are considered Works of the United States Government. However, the findings and conclusions presented in this paper are those of the authors and do not necessarily reflect the views of the NIH or the U.S. Department of Health and Human Services.

Appendix 1

Synthetic demonstration data

To construct synthetic data, we adapted the procedure described in Cui et al. (2022) for concurrent modeling. Let $i = 1, 2, \ldots, I$ index subject IDs and $j = 1, 2, \ldots, J$ index replicates (i.e. trials). We simulated data according to the following functional mixed model

$$Y_{i,j}(s) = \beta_0(s) + \gamma_{i,0}(s) + \texttt{Vel}_{i,j}(s)[\beta_1(s) + \gamma_{i,1}(s)] + \epsilon_{i,j}(s)$$

where we defined the components

- $Y_{i,j}(s)$: the observed photometry signal for animal i at trial j and time s;
- $\texttt{Vel}_{i,j}(s)$: the observed velocity for animal i at trial j and time s;
- $\beta_0(s)$: the functional intercept at time s across all trials and subjects;
- $\beta_1(s)$: the average change in mean signal associated with a one-unit increase in velocity at time s across all trials and subjects;
- $\gamma_{i,0}(s)$: the random functional intercept of mouse i at time s across all trials; and
- $\gamma_{i,1}(s)$: the random functional slope for mouse i at time s, i.e., the subject-specific perturbation to the population signal–velocity slope.

Let $\mathcal{S}$ be the functional domain, with size L. Velocity values were drawn from 0.00 to 5.00 seconds in increments of 0.05 seconds, i.e., $\mathcal{S} = \{0.00, 0.05, \ldots, 4.95, 5.00\}$, $|\mathcal{S}| = L = 101$. We sampled the vector of velocities across within-trial timepoints $\texttt{Vel}_{i,j} = [\texttt{Vel}_{i,j}(s_1), \ldots, \texttt{Vel}_{i,j}(s_L)]^T$ from the L-dimensional multivariate normal

$$\texttt{Vel}_{i,j} \sim \text{MVN}(\mathbf{0}, \Sigma + \text{diag}(0.2)), \quad \Sigma_{a,b} = \exp\left(\frac{-(a-b)^2}{2\ell^2}\right)\sigma^2, \sigma = 1, \ell = 10,$$

where we drew each vector $\texttt{Vel}_{i,j}$ independently and identically distributed (i.i.d.) across values of i and j. We defined fixed effect as

$$\beta_0(s) = -0.75 - 0.5\sin(0.5\pi s) - 0.5\cos(0.5\pi s)$$
$$\beta_1(s) = \phi\left(\frac{s-0.6}{0.1}\right) + \phi\left(\frac{s-0.2}{1}\right) + \phi\left(\frac{s-4}{1.5}\right),$$

where Φ is the standard Normal density function. We modeled random functional intercepts ($\gamma_{0,i}(s)$) and slopes ($\gamma_{1,i}(s)$) as the sum of two scaled orthonormal functions $\psi_1(s)$, $\psi_2(s)$. For every mouse $i \in \{1, \ldots, I\}$,

$$\gamma_{i,0}(s) = \sigma_B^2(s)\tilde{\gamma}_{i,0}(s), \quad \gamma_{i,1}(s) = \sigma_B^2(s)\tilde{\gamma}_{i,1}(s)$$
$$\sigma_B(s) = \texttt{SNR}_B \frac{\widehat{\text{SD}}(\beta_0(s) + \beta_1(s)\texttt{Vel}_{i,j}(s))}{\widehat{\text{SD}}(\tilde{\gamma}_{i,0}(s) + \tilde{\gamma}_{i,1}(s)\texttt{Vel}_{i,j}(s))}$$
$$\tilde{\gamma}_{i,0}(s) = c_{i,1}\psi_1(s) + c_{i,2}\psi_2(s), \quad \tilde{\gamma}_{i,1}(s) = c_{i,3}\psi_1(s) + c_{i,4}\psi_2(s)$$
$$\psi_1(s) = 1.5\sin(2\pi s) - \cos(2\pi s), \quad \psi_2(s) = \sin(4\pi s)$$
$$\mathbf{c}_i \sim \mathcal{N}(\mathbf{0}, [\text{diag}(3, 1.5, 0.75, 1.25)]),$$

where $\widehat{\text{SD}}$ is the empirical standard deviation and $\texttt{SNR}_B$ is a scaling parameter controlling the relative importance of fixed effects to subject-specific variability. Here, $\texttt{SNR}_B = 1$. We sampled the vectors $\mathbf{c}_i$ i.i.d. across subjects, i. We defined measurement noise $\epsilon_{i,j}(s)$ as

$$\epsilon_{i,j}(s) \sim \mathcal{N}(0, \sigma^2(s))$$
$$\sigma(s) = \texttt{SNR}_\sigma \widehat{\text{SD}}(\beta_0(s) + \gamma_{i,0}(s) + \texttt{Vel}_{i,j}(s)[\beta_1(s) + \gamma_{i,1}(s)])$$

and sampled $\epsilon_{i,j}(s)$ independently across mouse i, trial j, and time s. The scaling parameter $\texttt{SNR}_\sigma$ controls the relative importance of the combined fixed and random effects to the measurement noise. Here, $\texttt{SNR}_\sigma = 1$. Unlike simulations in Cui et al. (2022), $\sigma_B^2(s)$ and $\sigma^2(s)$ are functions, allowing for $\texttt{SNR}_B$ and $\texttt{SNR}_\sigma$ to be constant along the functional domain. Visualizations of the random and fixed effects are below, in Figure 1.

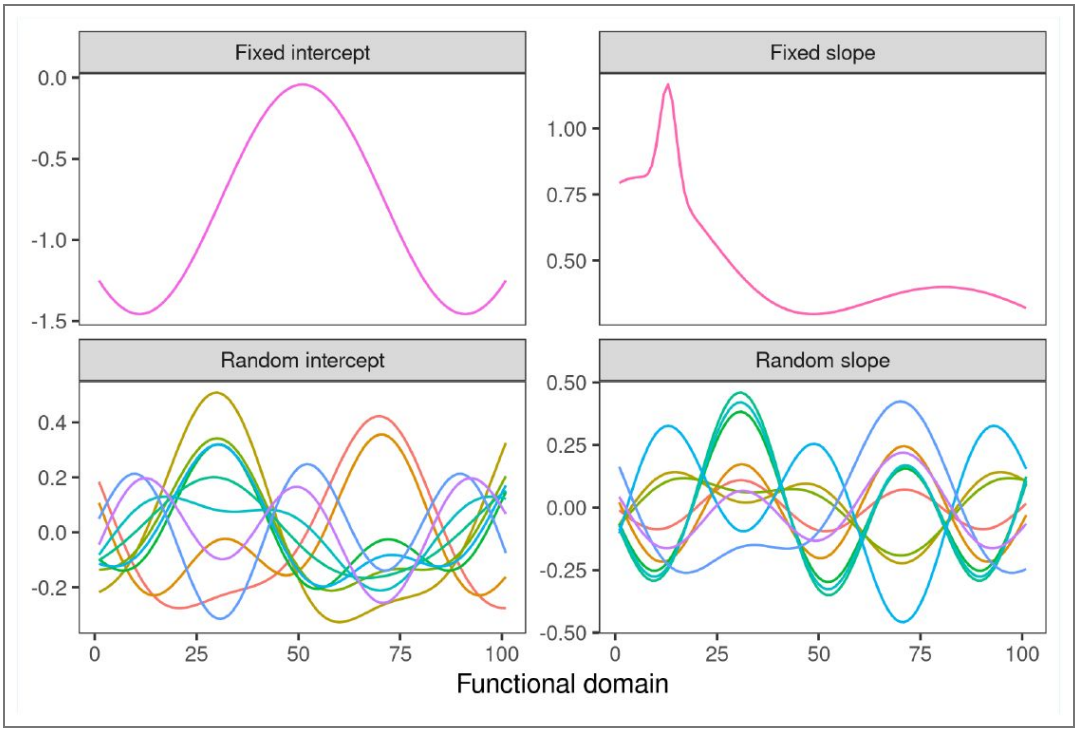

Appendix 1–figure 1. Functions corresponding to the fixed effects and a sample of 10 i.i.d. draws of subject-specific random effects. The fixed intercept $\beta_0(s)$ is the true relationship between signal and time when velocity is zero at time s, and the fixed slope $\beta_1(s)$ is the true relationship between signal and velocity at time s. The random intercept $\gamma_{i,0}(s)$ is individual perturbation of the fixed intercept for mouse i at time s, and the random slope $\gamma_{i,1}(s)$ is the individual perturbation of the fixed slope for mouse i at time s.

To create the data and fit the model shown in Figure 1, we generated $I = 40$ unique mice with $J = 40$ replicates each. For clarity, only 3 unique IDs and 10 replicates are shown in Figure 1-iB. The random effects shown in Figure 1Bii- are synthetic for visualization purposes, but the true random effects and instantaneous covariate recordings are shown below, in Figure 2.

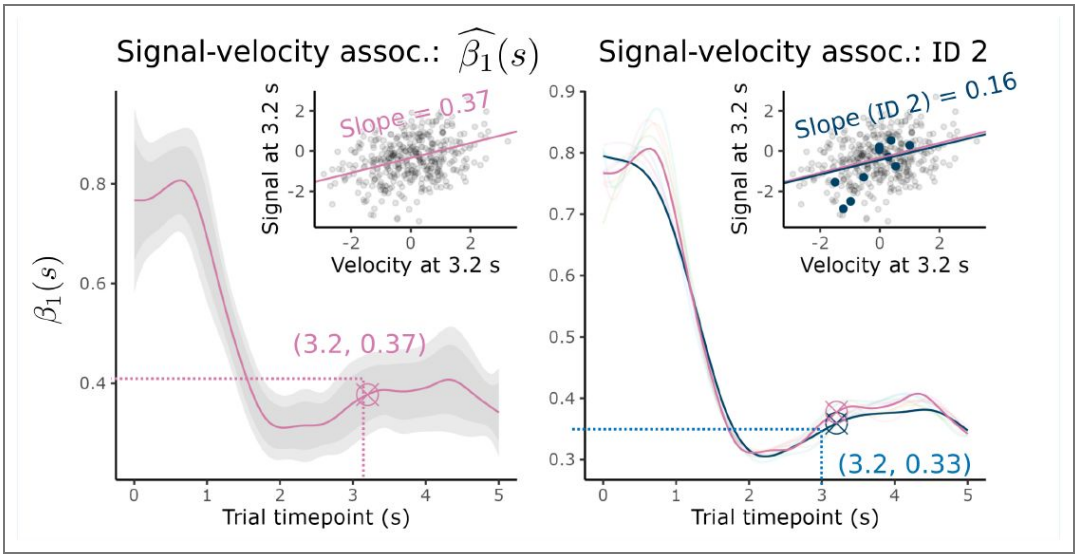

Appendix 1–figure 2. Data points in the insets correspond to the true values generated for the demonstration.

Appendix 2

95% Confidence interval coverage in simulations

We simulated data with the procedure described in Appendix 1. For results in Verification of method performance in simulations, we generated data according to the following mixed effects model:

$$Y_{i,j}(s) = \beta_0(s) + \gamma_{i,0}(s) + \texttt{Vel}_{i,j}(s)\beta_1(s) + \epsilon_{i,j}(s),$$

where the functional covariate, fixed effects, and random effects were defined in Appendix 1. We removed the random slope by setting $\gamma_{i,1}(s) = 0$ for all values of s.

Coverage with random slopes

We also examined coverage for simulated data that included random slope, i.e., with data generated according to the mixed effects model

$$Y_{i,j}(s) = \beta_0(s) + \gamma_{i,0}(s) + \texttt{Vel}_{i,j}(s)[\beta_1(s) + \gamma_{i,1}(s)] + \epsilon_{i,j}(s).$$

We found that the joint 95% CI coverage of cFLMM models fit to data simulated with random slopes was more sensitive to the magnitude of between-subject variability (i.e., $\texttt{SNR}_B$, the variance of the random effects). For example, in Figure 1, higher variance of the random effects was associated with lower joint coverage. The pointwise coverage tended to be far more robust to this parameter. We present simulations without a random slope in the main body to visualize changes in coverage as a function of $\texttt{SNR}_\sigma$.

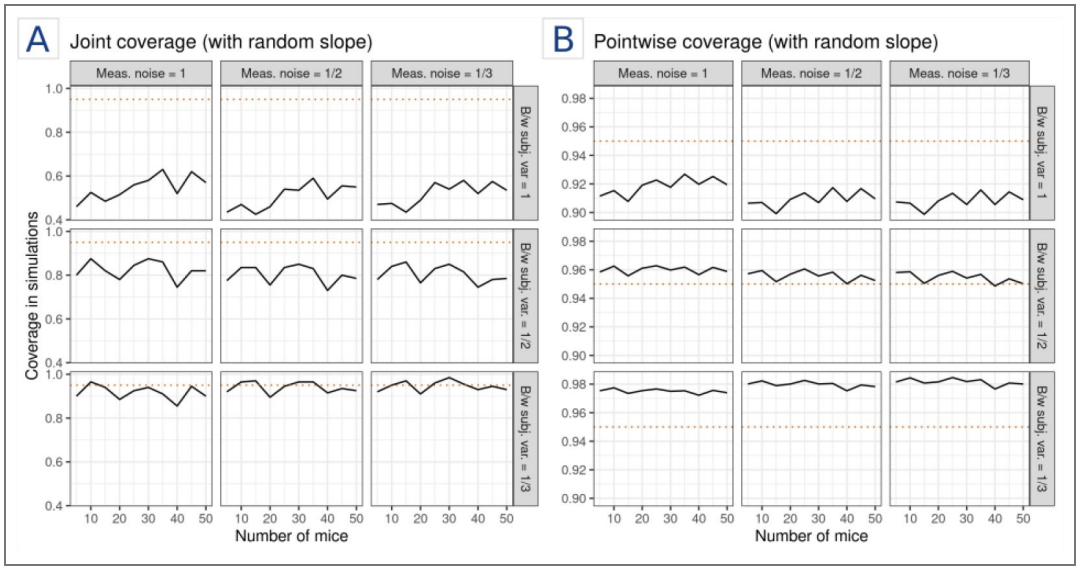

Appendix 2–figure 1. **Joint (A) and pointwise (B) coverage in simulations when incorporating a random slope.**

Visualization of signal-noise ratios

For visual reference, we generated synthetic photometry signals based on the simulation setup (Fig 2).

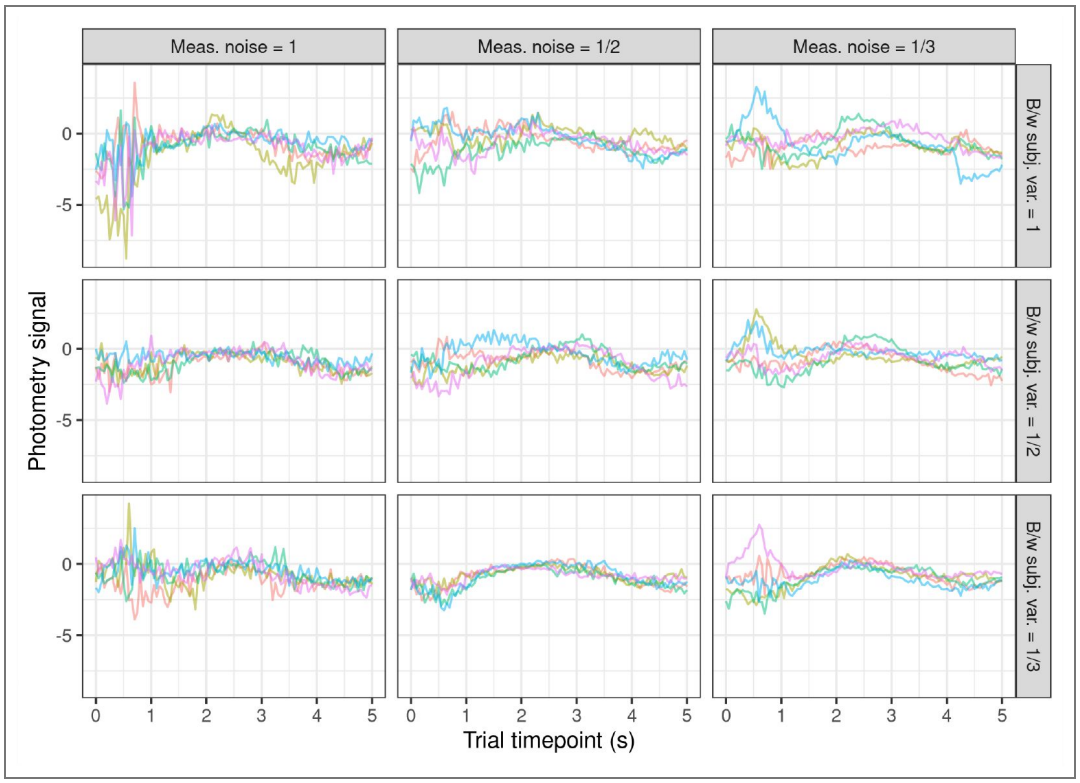

Appendix 2–figure 2. **Traces of synthetic photometry signals for five subjects with one observation each.**

Appendix 3

Additional fixed effects estimates

Although we incorporated non-functional fixed effects for trial and session into the model, we did not present or interpret these estimates in the main body of Modeling behaviors that change over the trial. There are slight differences in coefficient estimates for the fixed effects associated with trial number and session number. We focused on highlighting the particular changes in interpretation associated with exchanging the functional covariate $\texttt{Lick}_{i,j,l}(s)$ (which varies over trial timepoints) for the non-functional lick rate summary co-variate, $\texttt{LR}_{i,j,l}$ (which is a scalar value for each trial).

The magnitudes of the coefficient estimates vary between the cFLMM and ncFLMM models due to the difference in magnitude between the values of $\texttt{Lick}_{i,j,l}(s)$, which is binary (0 or 1), and $\texttt{LR}_{i,j,l}$, which usually takes values within [0, 0.2]. We can, however, still compare the shape and sign (i.e., positive or negative) of the effect estimates. Fixed effect estimates for trial number are consistent across all models, both in the shape of the coefficients and the width of the joint confidence bands. Estimates for session number are also consistent in shape between models, though ncFLMM models for $T = 0.5, 2.0$ have much wider joint confidence bands during early within-trial timepoints compared to cFLMM (Fig 1). This may be related to the use of lick rate as a summary statistic, as increased licking behavior does not immediately follow reward delivery (Fig 2A-i). This inconsistency may introduce additional variance into the coefficient estimates early in the trial. However, it is unclear why this affects confidence band estimates for session and not trial number or lick rate; it may be due to learning having a non-linear relationship with increasing session. We compare the lick covariate functional coefficient estimates in the main text.

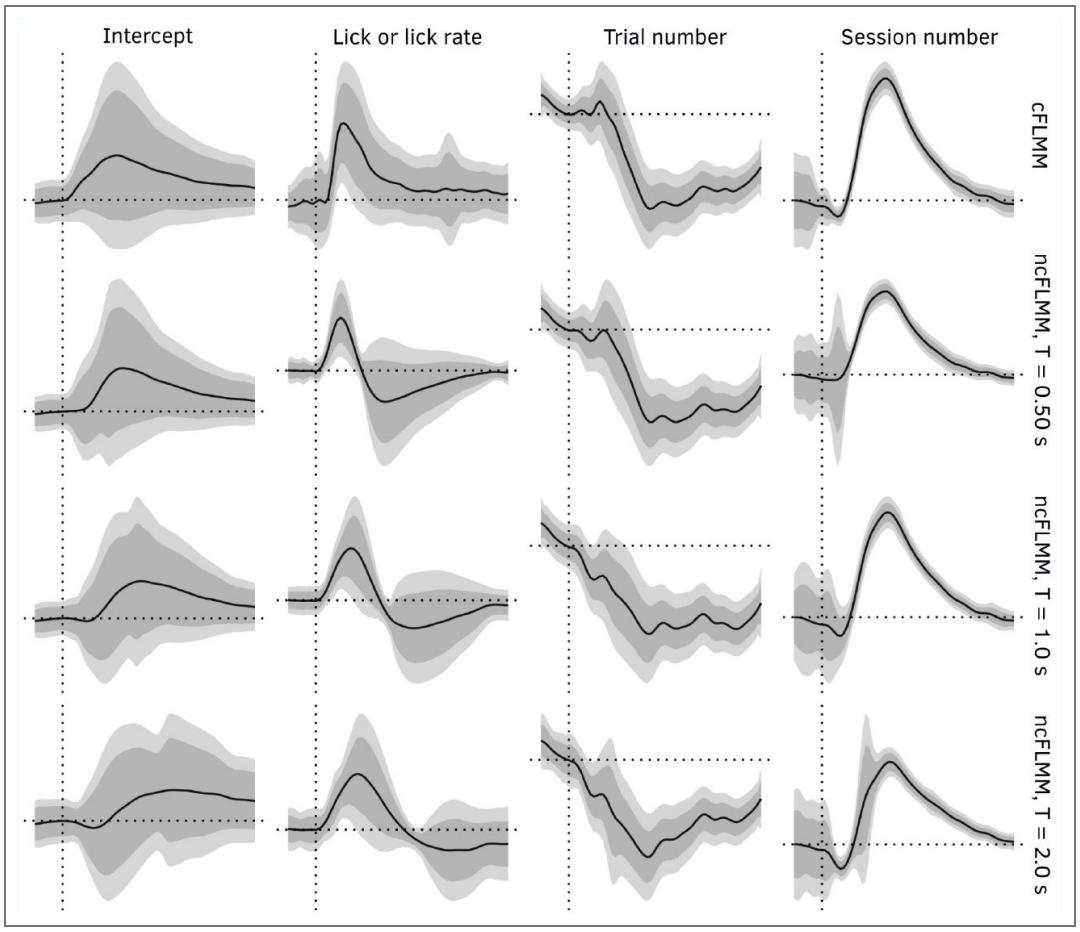

Appendix 3–figure 1. Point estimates and confidence intervals for all fixed effects included in the models compared in Modeling behaviors that change over the trial. Axes are omitted because the scale of the concurrent and non-concurrent models are different based on the covariate of lick or lick rate.

Appendix 4

Speeding up covariance calculation with method-of-moments

Discussion of speed-ups will refer to the three-step process of model fitting described in Box 1. When estimating covariance between fixed effects (Eqn. 3), the random effects covariance matrix $\mathbb{G}$ must be estimated from the data. To do so, we apply the method of moments estimator described in Greven et al. (2010), applied in Cui et al. (2022) for this functional mixed modeling estimation strategy, and extended in Loewinger et al. (2025) to general random effect specifications. Specifically, we calculate

$$\mathbb{E}\left[\{Y_{i,k}(s_1)-\mathbf{X}(s_1)_{i,k}^T\boldsymbol{\beta}(s_1)\}\{Y_{i,j}(s_2)-\mathbf{X}(s_2)_{i,j}^T\boldsymbol{\beta}(s_2)\}\right]=\sum_{t=1}^{q}\sum_{t=1}^{q}Z_{i,k,t}(s_1)Z_{i,j,v}(s_2)\mathrm{Cov}\left(\gamma_{i,t}(s_1),\gamma_{i,v}(s_2)\right) \quad (9)$$

where t, v are random-effect covariate indices and j, k are trial indices. We can then regress the residual produces onto the random effect covariate products. Compared to the method of moments estimator applied in the non-concurrent FLMM (Cui et al.,2022; Loewinger et al.,2025), we substitute $\mathbf{X}(s)$ for $\mathbf{X}$ and $\mathbf{Z}(s)$ for $\mathbf{Z}$ in each occurrence.

Although both the non-concurrent and concurrent case theoretically require the same number of calculations, in practice we can reduce the number of necessary calculations in the non-concurrent case as the design matrices are constant across the functional domain. After obtaining the fixed coefficient point estimates $\hat{\boldsymbol{\beta}}(s), \hat{\boldsymbol{\gamma}}(s)$ for each point s, the univariate models can be discarded in ncFLMM estimation.

In the concurrent case, however, we need to store the functional matrices $\mathbf{Z}(s)$, $\mathbf{X}(s)$ for all s for the variance estimation at Step 3. When incorporating even simple indicator variables for categorical random variables, the number of calculations needed to calculate the unique combinations of s_1, s_2 grows quadratically with respect to the size of the functional domain. We can, however, modify the estimator to work with only the row sums of the random effects, using an adaptation of the derivation described in *Appendix 3.1* of Loewinger et al. (2025). We briefly review the necessary adaptation for the cFLMM case here.

If q is the number of random effects in the model, let q^* be the number of unique random effect distributions, where $q^* \leq q$. For clarity, if we have some $r \in \{1, 2, ..., q^*\}$ corresponding to a categorical variable with r' groups, we have a corresponding set $\mathcal{I}_r \subseteq \{1, 2, ..., q\}$ of size $r' - 1$ indexing the columns in the random effect design matrix containing the indicator variables necessary to model r. Let r, m index the sets of random effects with the same distribution. We can then rewrite Equation 9 as

$$\begin{aligned}
&\sum_{t=1}^{q}\sum_{v=1}^{q} Z_{i,k,t}(s_1)Z_{i,j,v}(s_2)\mathrm{Cov}\left(\gamma_{i,t}(s_1),\gamma_{i,v}(s_2)\right)\\
&=\sum_{r=1}^{q^*}\sum_{m=1}^{q^*}\sum_{w\in\mathcal{I}_r}\sum_{b\in\mathcal{I}_m} Z_{i,k,w}(s_1)Z_{i,j,b}(s_2)\mathrm{Cov}\left(\gamma_{i,w}(s_1),\gamma_{i,b}(s_2)\right)\\
&=\sum_{r=1}^{q^*}\sum_{m=1}^{q^*}\left\{\sum_{w\in\mathcal{I}_r} Z_{i,k,w}(s_1)\left[\sum_{b\in\mathcal{I}_m} Z_{i,j,b}(s_2)\mathrm{Cov}\left(\gamma_{i,w}(s_1),\gamma_{i,b}(s_2)\right)\right]\right\}\\
&=\sum_{r=1}^{q^*}\sum_{m=1}^{q^*}\left[\sum_{w\in\mathcal{I}_r} Z_{i,k,w}(s_1)\right]\left[\sum_{b\in\mathcal{I}_m} Z_{i,j,b}(s_2)\right]\mathrm{Cov}\left(\gamma_{i,r}(s_1),\gamma_{i,m}(s_2)\right).
\end{aligned}$$

We derived the final equality by noting for random effects in the set $\mathcal{I}_r$, we have $\gamma_{r,i,w}(s) \overset{\text{i.i.d.}}{\sim} \mathcal{N}(0, \tilde{\sigma}_r^2(s))$, and thus $\mathrm{Cov}(\gamma_{r,i,w}(s_1), \gamma_{r,i,b}(s)) = \tilde{\rho}_{r,m}(s)$, where $\tilde{\rho}_{r,m}(s)$ is the same for all $w \in \mathcal{I}_r$, $b \in \mathcal{I}_m$. Thus, during Step 1, the matrices $\mathbf{Z}(s)$ can be reduced to a vector of row sums, summed across the vectors $\mathbf{Z}_{i,k}(s)$, saving both memory and computational time during the covariance estimation step.

Unfortunately, there are no similar simplifications for the $\mathbf{X}(s)$ in Equation 3 that we are aware of, and so these design matrices must be stored in memory until Step 3. Luckily, the matrices $X(s)$ tend to be far smaller than the $Z(s)$ and are thus usually manageable to store in memory. Moreover, the need to keep the $X(s)$ in memory is largely a byproduct of the choice to incorporate the smoothed estimates of coefficients in the variance estimation of Step 3. In future model development, it may be possible to parallelize Steps 1 to 3 across the functional domain and eliminate the need to store all L instances of $\mathbf{X}(s)$ simultaneously.

Additional information

Funding

Funder	Grant reference number	Author
HHS | National Institutes of Health (NIH)	ZIC MH002968	Francisco Pereira Gabriel Loewinger Alison Xin

Author ORCID iDs

Al W Xin: https://orcid.org/0000-0002-7954-8049
Erjia Cui: https://orcid.org/0000-0003-3576-2892
Francisco Pereira: https://orcid.org/0000-0003-2773-3426
Gabriel Loewinger: https://orcid.org/0000-0002-0755-8520

References

Cui E, Leroux A, Smirnova E, Crainiceanu CM (2022) Fast Univariate Inference for Longitudinal Functional Models. *Journal of Computational and Graphical Statistics* **31**:219-230 https://doi.org/10.1080/10618600.2021.1950006 | PubMed

Greven S, Crainiceanu C, Caffo B, Reich D. (2010) Longitudinal functional principal component analysis. *Electronic Journal of Statistics* **4**:1022-1054 https://doi.org/10.1214/10-EJS575

Jeong H, Taylor A, Floeder JR, Lohmann M, Mihalas S, Wu B, Zhou M, Burke DA, Namboodiri VMK (2022) Mesolimbic dopamine release conveys causal associations. *Science* **378**:eabq6740 https://doi.org/10.1126/science.abq6740

Loewinger G, Cui E, Lovinger D, Pereira F. (2025) A statistical framework for analysis of trial-level temporal dynamics in fiber photometry experiments. *eLife* **13**:RP95802 https://doi.org/10.7554/eLife.95802

Machen B, Miller SN, Xin A, Lampert C, Assaf L, Tucker J, Pereira F, Loewinger G, Beas S. (2025) The encoding of interoceptive-based predictions by the paraventricular nucleus of the thalamus D2+ neurons. *bioRxiv* https://doi.org/10.1101/2025.03.10.642469

Pinheiro J, Bates D, R Core Team (2025) nlme: Linear and Nonlinear Mixed Effects Models R package. version: v.3.1-168 https://CRAN.R-project.org/package=nlme

Scheipl F, Gertheiss J, Greven S. (2016) Generalized functional additive mixed models. *Electronic Journal of Statistics* **10**:1455-1492 https://doi.org/10.1214/16-EJS1145

Peer reviews

Reviewer #1 (Public review):

Summary:

The authors aimed to extend a prior fiber photometry analysis process they developed by incorporating the new ability to determine instantaneous, within trial, relationships between the photometry signal and continuously changing variables. They present solid evidence via simulations and example use cases from published datasets highlighting that their approach can capture instantaneous relationships. Overall, while they make a compelling case that this approach is less biased and more insightful, the implementation for many experimentalists remains challenging enough and may limit widespread adoption by the community.

Strengths:

This work builds on prior efforts to analyze photometry signals in a less biased and more statistically sound way. This work incorporates a very important aspect by avoiding the need to summarize individual trials with singular behavioral variables and instead allows for interactions with continuously changing variables to be investigated. The knowledge and expertise of the authors and the presentation provide strong validity and strength to the work. Examples from prior studies in the field are a necessary and important component of the work.

Weaknesses:

While use cases are provided from prior data, a clearer presentation of how common implementations in the field are performed (i.e. GLM) and how one could alternatively use the cFLMM approach would help. Otherwise, most may continue using common approaches of Pearson's correlations and GLMs.

https://doi.org/10.7554/eLife.109428.1.sa3

Reviewer #2 (Public review):

The paper presents a regression-based approach for analysing fiber photometry data termed Concurrent Functional Mixed Models (cFLMMs). The approach works by fitting linear mixed effect models separately to each time point in trial aligned data, then applying smoothing to the model coefficients (betas), and computing confidence intervals. The method extends the authors previous work on using FLMMs for photometry data analysis by allowing for the inclusion of predictors whose value changes across timepoints within a trial, rather than just from trial to trial. As fiber photometry is a rapidly expanding field, developing principled methods to analyse photometry data is valuable, particularly as the authors have released an R package that implements their method to facilitate their use by other groups. The basic FLMM approach for using mixed effects models to analyse trial aligned photometry data, detailed by the authors in their previous manuscript (Loewinger et al. 2025, doi: 10.7554/eLife.95802) appears valuable. The aim of incorporating variables that change within trial into this framework is interesting, and the technical implementation appears to be rigorous. However, I have some reservations as to whether the way in which variables that change within trial have been integrated into the analysis framework is likely to be widely useful, and hence how impactful the additional functionality of cFLMM relative to the previously published FLMM will be.

In the original FLMM approach, where predictors change only from trial-to-trial, fitting separate regressions at each timepoint generates a timeseries of betas is for each predictor, indicating when and how the predictor explained variance across the trial. This makes a lot of sense and is widely used in neuroscience data analysis. In extending this approach to incorporate variables that change within trial, the authors have used the same method of fitting separate regression models at each timepoint, to obtain a timeseries of betas for each predictor. It is less clear that this approach makes sense for variables that change within trial. This is because the resulting betas only capture how variation in the predictor across trials at a given timepoint explains variance in the signal, but does not capture effects of variation in the predictor across timepoints within trials. This partitioning of variance in the predictor into a between-trial component whose effect on the signal is modelled, and a within-trial component whose effect on the signal is not, is artificial in many experiment designs, and may yield hard to interpret results.

Consider e.g. the experimental condition considered in Figure 3, taken from Machen et al. 2025 (doi: 10.1101/2025.03.10.642469) in which mice ran down a linear track to collect rewards. In analysing such data, one might want to know how neural activity covaried with the animal's position, but as this variable changes strongly within trial but will have a similar time-course across trials, the cFLMM analysis approach will not work to quantify these effects. This is because variance attributed to position would not capture how neural activity covaried with changes in the animals position within trial, but rather how neural activity covaried with changes in the animals position from trial-to-trial at a given timepoint, which could occur due to e.g. trial-to-trial differences in latency to start moving or running speed. As such, although significant effects of 'position' might be observed, they would not capture covariation between position and neural activity in a straightforwardly interpretable way.

It is therefore not obvious to me that incorporating variables that change within trial into an analysis framework that runs separate regressions at each timepoint in trial aligned data is likely to be widely useful. If scientific questions require understanding how neural activity covaries as a function of variables that change both within and across trials, an alternative approach would be to run a single regression analysis across all timepoints, and capture the extended temporal responses to discrete behavioural events by using temporal basis functions convolved with the event timeseries. This provides a very flexible framework for capturing covariation of neural activity both with variables that change continuously such as

position, and discrete behavioural events such as choices or outcomes, while also handling variable event timing from trial-to-trial.

One way that cFLMM is used in the manuscript is to handle variable timing of trial events in trial aligned data. In the Machen et al. data, the time when the animal reaches the reward varies from trial to trial, and this is represented in the cFLMM analysis by a binary variable which changes value at this timepoint. From the resulting beta coefficient timeseries (Figure 3C) it is not straightforward to understand how neural activity changed as the subject approached and then received the reward. A simpler approach to quantify this, which I think would have yielded more interpretable coefficient timeseries would have been to align activity across trials on when the subject obtained the reward, rather than on the start of the trial, allowing e.g. the effect of reward type to be visualised as a function of time relative to reward delivery, and hence to see the differential effects during approach vs consumption. More broadly, handling variable trial timing in analyses like FLMM which use trial aligned data, can be achieved either by separately aligning the data to different trial events of interest or by time warping the signal to align multiple important timepoints across trials. It is not obvious that using cFLMM with binary indicator variables that indicate when task states changed will yield a clearer picture of neural activity than these methods.

It may be that I am missing some key strengths of cFLMM relative to the other approaches I have outlined, or that there are applications where this approach to implementing within-trial variable changes is a natural formalism. However my impression is that while cFLMM represent a technical advance, it is not clear how widely useful the model formalism will be.

https://doi.org/10.7554/eLife.109428.1.sa2

Reviewer #3 (Public review):

Summary:

This work is an extension of their previous study (Loewinger et al 2025) describing a statistical framework for the analysis of photometry data using functional linear mixed models with joint confidence intervals, together with an open-source tool implemented in R. The present study extends it by adding the possibility of using 'concurrent' variables (variables that change within a trial) as regressors, for example, capturing the change of speed at each timepoint in the trial. The main claim is that using 'concurrent' regressors can identify associations between signal and behavior that could not be captured by 'non-concurrent' regressors (the value for a regressor on a specific trial is the same for each timepoint), which could lead to misleading conclusions. While the motivation for using time-varying covariates is useful and supported by previous literature (using fixed-effects models, although not cited in this manuscript), the reanalysis of previous studies does not clearly prove the benefit of using concurrent regressors as opposed to non-concurrent, and some of the results are difficult to interpret.

Strengths:

• The motivation for using time-varying covariates is well supported by previous literature using them on fixed-effects models, and here the authors are extending it to mixed-effects models.

• The authors have included this new functionality in their previous open-source R package.

Weaknesses:

• The main weakness of this study is that it is not clear what the conceptual or methodological advance of this work is. As it is written, the manuscript focuses on showing how concurrent regressors offer interpretation advantages over non-concurrent regressors. While the benefit

of such time-varying regressors is supported by previous literature (e.g., Engelhard et al., 2020), it is not clear whether the examples provided in the current study clearly support the advantage of one over the other, especially in the reanalysis of Machen et al. (2025), where the choice of regressors is confusing. In this specific example, if the question is about speed and reward type, why variables such as latency to reward or a binary 'reward zone vs corridor' (RZ) regressors are used instead of concurrent velocity (or peak velocity - in the case of the non-concurrent model)? Furthermore, if timing from trial start to reward collection is variable, why not align to reward collection, which would help in the interpretation of the signal and comparison between methods? Furthermore, while for the non-concurrent method, the regressors' coefficients are shown, for the concurrent one, what seems to be plotted are contrasts rather than the coefficients. The authors further acknowledge the interpretational difficulties of their analysis.

• Because the relation between behavioral variables and neuronal signal is not instantaneous, previous literature using fixed effects uses, for example, different temporal lags, splines, and convolutional kernels; however, these are not discussed in the manuscript.

• From the methods, it seems that in the concurrent version of fastFMM, both concurrent and non-concurrent regressors can be included, but this is not discussed in the manuscript.

• The methodological advance is not clearly stated, apart from inputting into fastFMM a 3D matrix of regressors x trial x timepoint, instead of a 2D matrix of regressors x trial.

• This manuscript is neither a clear demonstration of the need for concurrent variables, nor a 'tutorial' of how to use fastFMM with the added extension.

https://doi.org/10.7554/eLife.109428.1.sa1

Author response:

Common responses:

We thank the editors for considering our paper and the reviewers for their thoughtful and detailed feedback. Based on the comments, we will revise our manuscript to better describe how our approach differs from modeling strategies that are common in the field. We also aim to elaborate on the advantages of fastFMM and what scientific questions it is designed to answer. Finally, we will provide more background on our example analyses and the interpretation of the results.

Within this response, “within-trial timepoints”, “time-varying predictors/behaviors”, and “signal magnitude” are used as specific examples of the general concepts of functional domain”, “functional co-variates”, and “functional outcome”, respectively. To make statements or examples more concrete, we may use the former neuroscience-specific terms when making general claims about functional models.

- ncFLMM, cFLMM: non-concurrent or concurrent functional linear mixed models.

- FUI: fast univariate inference. An approximation strategy to perform FLMM Cui et al. (2022).

- fastFMM the R package that implements FUI.

- CI confidence interval.

Before specific line-by-line responses, we provide a brief comparison between cFLMM and fixed effects encoding models. All three reviewers suggested that fixed effects models could be an existing alternative to cFLMM (Reviewer 1 (1B), Reviewer 2 (2C), Reviewer 3 (3A)). Their shared comments highlight that our revision should articulate the advantages and applications of cFLMM relative to existing analysis strategies.

Functional regression methods like cFLMM produce functional coefficient estimates that quantify how the magnitude of predictor-signal associations evolve across an ordered functional domain such as within-trial timepoints. Standard scalar outcome regression methods, like the GLMs specified in Engelhard et al. (2019), model these associations and their corresponding coefficients as fixed across the functional domain. While GLM encoding models may include time-varying predictors, these analysis strategies do not model the predictor–signal association as changing over the functional domain.

Moreover, encoding models are less suited to hypothesis testing in clustered or longitudinal settings (e.g., repeated-measures datasets) and yield regression coefficient estimates that are only interpretable with respect to the units of the basis functions. In contrast, cFLMM provides time-varying coefficient estimates that are interpretable as statistical contrasts in terms of the original variables and produces hypothesis tests in clustered settings. cFLMM can be applied to datasets that define covariates in terms of the same flexible representations of covariates used in encoding models; this is a modeling choice rather than a methodological characteristic.

The remainder of this provisional author response will respond to reviewers' concerns line-by-line, approximately in the order they appear.

> ***Reviewer #1 (Public review):***

We thank Reviewer 1 for their comments, especially their efforts to provide first-hand experience with loading and applying fastFMM. We hope that recent improvements to fastFMM's public release and vignettes address Reviewer 1's concerns about ease-of-use.

> *(1A) Overall, while they make a compelling case that this approach is less biased and more insightful, the implementation for many experimentalists remains challenging enough and may limit widespread adoption by the community.*

We believe the reviewer may have experimented with an old version of fastFMM, so their experience may not reflect recent rewrites and improvements. fastFMM v1.0.0+ is now stable, validated on CRAN, and contains new example data and step-by-step tutorials. We designed fastFMM's model-fitting code to be similar to common GLM packages in R to reduce the learning curve for new users.

> *(1B) …a clearer presentation of how common implementations in the field are performed (i.e. GLM) and how one could alternatively use the cFLMM approach would help.*

We will provide a clearer description of existing methods in the revised manuscript. Briefly, inference with fastFMM can accommodate large datasets that contain clustered data, repeated measures, or complex hierarchical effects, e.g., experiments with multiple animals and multiple trials per animal. When encoding models are fit to each cluster (e.g., animal, neuron) separately, we are not aware of a principled method to pool these cluster-specific models together to quantify uncertainty or yield an appropriate global hypothesis test.

> ***Reviewer #2 (Public review):***

Reviewer 2's thoughtful feedback helped structure our points in the common response above, which we will refer to when applicable. In our response, we aim to clarify the problems that cFLMM solves and characterize the advantages in interpretability.

> *(2A) The aim of incorporating variables that change within trial into this framework is interesting, and the technical implementation appears to be rigorous. However, I have some reservations as to whether the way in which variables that change within trial have been integrated into the analysis framework is likely to be widely useful, and hence how impactful the additional functionality of cFLMM relative to the previously published FLMM will be.*

We hope that the common response addresses these concerns. We were motivated to provide a concurrent extension of fastFMM based on our experience with statistical consulting in neuroscience research. Questions that benefit from a functional approach are common and often not adequately modeled with a non-concurrent approach, such as the variable trial length analysis we describe below.

> *(2B) It is less clear that this approach makes sense for variables that change within trial… This partitioning of variance in the predictor into a between-trial component whose effect on the signal is modeled, and a within-trial component whose effect on the signal is not, is artificial in many experiment designs, and may yield hard to interpret results.*

We thank Reviewer 2 for highlighting a point that we did not adequately explain and that we will address further in the revision. The pointwise and joint CIs estimated by fastFMM account for uncertainty in the coefficient estimates due to variation in the predictors across within-trial timepoints. cFLMM targets a statistical quantity, or estimand, that is defined by trial timepoint specific effects, so the first step of our estimation strategy fits separate pointwise mixed models. However, models from every within-trial timepoint are then combined to calculate uncertainty and smooth the coefficient estimates. Thus, the widths of the pointwise and joint CIs depend on the estimated between-timepoint covariance and a smoothing penalty. Loewinger et al. (2025a) provides further details in Appendices 2 and 3, describing the covariance structure and detailing the power improvements of FUI compared to multiple-comparisons corrections.

Other functional regression estimation strategies jointly fit the entire model with a single regression, e.g., functional generalized estimating equations Loewinger et al (2025b). However, these methods use basis expansions of the coefficients. In contrast, the encoding models mentioned in 2C below and Reviewer 3 (3A) apply basis-expansions of the covariates, and the resulting model does not capture how signal–covariate associations evolve across some functional domain. Although the first stage in the fastFMM approach fits pointwise linear models, this is only one of three steps in the estimation strategy. fastFMM yields coefficient estimates comparable to those that would be obtained from functional regression estimation strategies that jointly estimate the functional coefficients in a single regression. We mention this to distinguish between the target statistical quantity (functional coefficients) and the estimation strategy (pointwise vs. joint).

> *(2C) …an alternative approach would be to run a single regression analysis across all timepoints, and capture the extended temporal responses to discrete behavioural events by using temporal basis functions convolved with the event timeseries. This provides a very flexible framework for capturing covariation of neural activity both with variables that change continuously such as position, and discrete behavioural events such as choices or outcomes, while also handling variable event timing from trial-to-trial.*

Our understanding is that the suggested approach aims to quantify the association between the outcome and within-trial patterns in covariates. This is a great question and we will

incorporate a discussion of this into the revision. However, temporal basis functions convolved with the covariate time series cannot directly characterize these relationships. Encoding models can detect the contribution of predictors to neural signals while remaining agnostic to the precise relationship, but this flexibility can come at the cost of interpretability. The coefficients of the convolutions may not be translatable into a clear statistical contrast in terms of the original covariates.

In our paper, we provide examples of cFLMM models with simple signal-covariate relationships. The coefficient estimates quantify the expected change in signal given a one unit change in the original predictors. Let $Y(s)$ be the outcome and $X(s)$ be some covariate at within-trial timepoint s. For brevity, we will suppress subject/trial indices and random effects in the following notation. The coefficient at time point s can be captured by the generic mean model

$$\mathbb{E}[Y(s) \mid X(s) = 1] - \mathbb{E}[Y(x) \mid X(s) = 0].$$

In contrast, the change in signal associated with patterns in within-trial covariates can be written as

$$\mathbb{E}[Y(s_1) \mid X(s_2) = 1] - \mathbb{E}[Y(s_1) \mid X(s_2) = 0]$$

for all pairs of timepoints s_1, s_2. While simple lagged or offset outcome-predictor associations can be incorporated as covariates in cFLMM, the approach does not capture all within-trial timepoints s_1, s_2. Encoding models also do not target the above estimand. Instead, a full function-on-function regression could estimate the above. This topic can be incorporated into our revision and may be a future line of inquiry.

> *(2D) In the Machen et al. data…From the resulting beta coefficient timeseries (Figure 3C) it is not straightforward to understand how neural activity changed as the subject approached and then received the reward. A simpler approach to quantify this, which I think would have yielded more interpretable coefficient timeseries would have been to align activity across trials on when the subject obtained the reward. More broadly, handling variable trial timing in analyses like FLMM which use trial aligned data, can be achieved either by separately aligning the data to different trial events of interest or by time warping the signal to align multiple important timepoints across trials.*

In this experiment, mice waited in a trigger zone, ran through a linear corridor, then received a food reward in the reward delivery zone of either water or strawberry milkshake Machen et al. (2026). Mice received different rewards between sessions but the same reward within all trials of a given session. This design complicated the analysis, as the reward type produced prominent differences in average latency (water: 3.3 seconds, milkshake: 2.0 seconds). The authors wanted to disentangle whether mean differences in the signal across reward types reflected differences in motivation to obtain the reward or differences in reaction to reward receipt.

We agree that performing a reward-aligned analysis would be an intuitive approach to visualize the differences in average signal for mice that received milkshake compared to water. In fact, we provide a ncFLMM reward-aligned analysis in Figure S1 of Machen et al. (2025). We will add this analysis to the revision and thank the reviewer for the suggestion. We emphasize, however, that this method answers a different question. It does not identify how the signal change associated with receiving the milkshake evolves with respect to latency, especially if the relationship is non-linear. Time warping faces similar obstacles in this setting, especially since sufficiently flexible curve registration can induce similarity due purely to noise. Generally, time warping does not lend itself to hypothesis testing as it is unclear how to propagate uncertainty from the time warping model into final hypothesis tests.

We believe cFLMM is an appropriate choice for the specific question, and we will revise the manuscript to better reflect its advantages. The functional coefficient estimates in Figures 3C-iii and 3C-iv provide insights that are not possible to derive from the proposed alternatives. For example, we can infer that for short latencies, we do not see a significant difference in signal magnitude for mice receiving water and mice receiving the milkshake. However, for latencies longer than around 2 seconds, receiving the milkshake is associated with an additional positive change in signal. We agree that we should make Figure 3C and the accompanying discussion more clear and thank Reviewer 2 for their feedback on interpretation.

> ***Reviewer 3 (Public review):***
>
> *(3A) ...it is not clear what the conceptual or methodological advance of this work is. As it is written, the manuscript focuses on showing how concurrent regressors offer interpretation advantages over non-concurrent regressors. While the benefit of such time-varying regressors is supported by previous literature (e.g., Engelhard et al., 2020), it is not clear whether the examples provided in the current study clearly support the advantage of one over the other...*

We assume Reviewer 3 is referencing “Specialized coding of sensory, motor and cognitive variables in VTA dopamine neurons Engelhard et al. (2019). We hope that the Common response sufficiently contrasts the settings where each approach can be applied. Because these models have different goals and assumptions, they are appropriate for answering different questions.

> *(3B) In this specific example, if the question is about speed and reward type, why variables such as latency to reward or a binary “reward zone vs corridor” (RZ) regressors are used instead of concurrent velocity (or peak velocity - in the case of the non-concurrent model)? Furthermore, if timing from trial start to reward collection is variable, why not align to reward collection, which would help in the interpretation of the signal and comparison between methods? Furthermore, while for the non-concurrent method, the regressors' coefficients are shown, for the concurrent one, what seems to be plotted are contrasts rather than the coefficients. The authors further acknowledge the interpretational difficulties of their analysis.*

Thank you for pointing out that we were not clear. This was mentioned by multiple reviewers and highlights the need to elaborate on our motivation in the revision. In this example, we wanted to investigate the change in signal-reward association as a function of within-trial timepoints, not the association between instantaneous velocity and the signal. “Slow” or “fast” means “mouse with below or above average latency”. We ask you to please refer to Reviewer 2 (2C) where we discuss why event alignment is an insufficient correction.

The functional coefficient estimates in Figure 3C are interpreted as contrasts because the fixed effect coefficients capture the difference in expected signal between strawberry milkshake and water along the functional domain. An advantage of cFLMM is that it is easy to specify models in which the coefficients correspond to interpretable contrasts of the signal across conditions. The coefficient estimate shown in Figure 3B-ii also corresponds to a contrast because the estimates capture the difference in mean signal from strawberry milkshake and water. Equations (7) and (8) in the section “Materials and methods” and sub-section “Variable trial length analysis” provide additional details on the fixed effect coefficients. Based on this confusion, we will convert the two 1 x 4 sub-plots of 3B and 3C into two 2 x 2 sub-plots to avoid unintended direct comparisons.

To contextualize how we “acknowledge the interpretational difficulties of [our] analysis”, we stated that a non-concurrent FLMM attempting to control for a time-based covariate is

difficult to interpret. The concurrent FLMM provides a straightforward interpretation directly related to the question of interest, which we discuss above in Reviewer 2 (2D).

> *(3C) Because the relation between behavioral variables and neuronal signal is not instantaneous, previous literature using fixed effects uses, for example, different temporal lags, splines, and convolutional kernels; however, these are not discussed in the manuscript.*

Thank you for this suggestion. All three reviewers raised this topic (see Reviewer 1 (1B), Reviewer 2 (2C), and the Common responses), and we will incorporate our response in the revision.

> *(3D) From the methods, it seems that in the concurrent version of fastFMM, both concurrent and non-concurrent regressors can be included, but this is not discussed in the manuscript.*

This is an important point that we mentioned implicitly. In our cFLMM specification of the Jeong et al. (2022) model, "we incorporated trial-specific covariates for trial number and session, modeling these as increasing numerical values rather than identical categorical variables", which are also plotted in Appendix 3. In Box 1, "if the functional covariate of interest is a scalar constant across the domain, the models fit by the concurrent and non-concurrent procedure are identical". We will explicitly point out that cFLMM can perform inference on combinations of functional and constant covariates.

> *(3E) The methodological advance is not clearly stated, apart from inputting into fastFMM a 3D matrix of regressors x trial x timepoint, instead of a 2D matrix of regressors x trial.*

Prior to our work described in this Research Advance, it was not obvious that the existing approximation approach in fastFMM could be generalized to cFLMM. During the writing of the article, a fastFMM user reached out for help with producing pseudo-concurrent FLMMs by duplicating rows in a nonconcurrent model, which both underscores the unmet need for cFLMMs and the difficulty in fitting them with available tools.

The "under-the-hood" differences are described in Appendix 4. Concurrent FLMM with fast univariate inference was theoretically possible as early as Cui et al. (2022). The univariate step was straightforward, but guaranteeing "fast" and "inference" was not. We needed to verify, for example, that the method-of-moments estimation of the random effects covariance matrix generalized to cFLMM, which is not a trivial step. Characterizing whether the method achieved asymptotic coverage required extensive simulation studies (Figure 4, Appendix 2). Future work may focus on fully characterizing the asymptotic convergence in high noise or high complexity regimes.

> *(3F) This manuscript is neither a clear demonstration of the need for concurrent variables, nor a 'tutorial' of how to use fastFMM with the added extension.*

We hope that the Common responses clarifies how cFLMM compares to existing approaches and fills a gap in the data analysis landscape for neuroscience. The fastFMM R package vignettes contain example analyses, and we intend for these files to be work in tandem with the manuscript. To provide more guidance for interested analysts, we can explicitly reference these tutorials within the revision.

Planned revisions

The following summary is not exhaustive.

Writing additions:

Per 1B, 2C and 3A, the Common responses will be incorporated in the revision.

Per 2B, we will discuss function-on-function regression and explore how to estimate statistical contrasts for complex within-trial relationships. Relatedly, we will clarify that the CIs in fastFMM are constructed using an estimate of the within-trial covariance of the predictors, and clarify the definition of pointwise and joint CIs.

Per 3D, we will explicitly state that concurrent FLMMs can include covariates that are constant over within-trial timepoints.

Though we cannot prescribe a universally correct model selection procedure, we will mention that AIC, BIC, and other summary statistics can inform the specification of the random effects.

Analysis modifications:

Parts of Appendix 3 may be included in Figure 2 to directly address the question investigated by Jeong et al. (2022) and Loewinger et al (2024).

When discussing Machen et al. (2025) data, the supplementary analysis with reward-aligned ncFLMM models might be added to clarify the ncFLMM/cFLMM difference.

Per \ref{rvw2:encoding}, the additional analysis aimed at disentangling latency and reward in Machen et al.'s variable trial length data may be incorporated as an additional sub-figure in Figure 3.

Aesthetic changes:

Figure 3 will be reorganized to avoid unintended direct comparisons between the coefficients of the non-concurrent and concurrent model.

Citations for Machen et al. (2026) will be updated to reflect publication of the preprint.

The version number for fastFMM will be updated.

References

Cui E, Leroux A, Smirnova E, Crainiceanu CM. Fast Univariate Inference for Longitudinal Functional Models. Journal of Computational and Graphical Statistics. 2022; 31(1):219–230. *https://doi.org/10.1080/10618600.2021.1950006*, doi: 10.1080/10618600.2021.1950006, pMID: 35712524.

Engelhard B, Finkelstein J, Cox J, Fleming W, Jang HJ, Ornelas S, Koay SA, Thiberge SY, Daw ND, Tank DW, Witten IB. Specialized coding of sensory, motor and cognitive variables in VTA dopamine neurons. Nature. 2019 Jun; 570(7762):509–513. *https://www.nature.com/articles/s41586-019-1261-9*, doi: 10.1038/s41586-019-1261-9.

Jeong H, Taylor A, Floeder JR, Lohmann M, Mihalas S, Wu B, Zhou M, Burke DA, Namboodiri VMK. Mesolimbic dopamine release conveys causal associations. Science. 2022; 378(6626):eabq6740. *https://www.science.org/doi/abs/10.1126/science.abq6740*, doi: 10.1126/science.abq6740.

Loewinger G, Cui E, Lovinger D, Pereira F. A statistical framework for analysis of trial-level temporal dynamics in fiber photometry experiments. eLife. 2025 Mar; 13:RP95802. doi: 10.7554/eLife.95802.

Loewinger G, Levis AW, Cui E, Pereira F. Fast Penalized Generalized Estimating Equations for Large Longitudinal Functional Datasets. ArXiv. 2025 Jun; p. arXiv:2506.20437v1. *https://pmc.ncbi.nlm.nih.gov/articles/PMC12306803/*.

Machen B, Miller SN, Xin A, Lampert C, Assaf L, Tucker J, Herrell S, Pereira F, Loewinger G, Beas S. The encoding of interoceptive-based predictions by the paraventricular nucleus of the thalamus D2R+ neurons. iScience. 2026 Jan; 29(1):114390. doi: 10.1016/j.isci.2025.114390.

https://doi.org/10.7554/eLife.109428.1.sa0